Submitted to Journal of Low Temperature Physics

LBL-4552
Preprint

TUNNEL JUNCTION DC SQUID: FABRICATION, OPERATION, AND PERFORMANCE

John Clarke, Wolfgang M. Goubau, and Mark B. Ketchen

March 1975

Prepared for the U. S. Energy Research and Development Administration under Contract W-7405-ENG-48

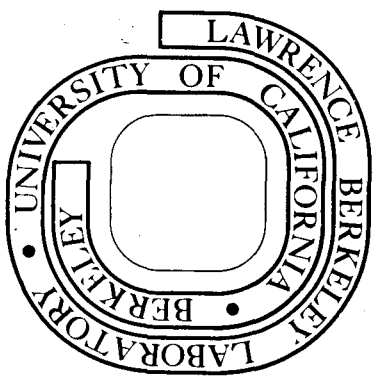

DISCLAIMER

TUNNEL JUNCTION DC SQUID: FABRICATION, OPERATION, AND PERFORMANCE

John Clarke, Wolfgang M. Goubau, and Mark B. Ketchen
Department of Physics, University of California, and
Materials and Molecular Research Division,
Lawrence Berkeley Laboratory, Berkeley, Calfornia 94720

ABSTRACT

We describe the theory, fabrication, operation, and performance of a cylindrical dc SQUID made with shunted Nb-NbO_x-Pb Josephson tunnel junctions. The SQUID is current-biased at a non-zero voltage, and modulated with a 100kHz flux. The 100kHz voltage developed across the SQUID is amplified by a cooled, resonant LC circuit that optimally couples the SQUID impedance to the input of a room temperature FET preamplifier. The SQUID is operated in a flux-locked loop with a dynamic range in a 1 Hz bandwidth of $\pm 3 \times 10^6$. The 3dB roll-off frequency for the loop response is typically 2kHz, and the slewing rate is generally $2 \times 10^4 \phi_o s^{-1}$. A typical flux noise power spectrum for a SQUID at 4.2K in a superconducting shield is presented. Above 2×10^{-2} Hz the spectrum is white and has an rms value of $3.5 \times 10^{-5} \phi_o Hz^{-\frac{1}{2}}$. The white noise is intrinsic to the sensor and is close to the theoretical limit set by Johnson noise in the shunts. At lower frequencies, the power spectrum is approximately

$10^{-10}(1\text{Hz}/f)\phi_o^2\text{Hz}^{-1}$, where f is the frequency. This value is approximately two orders of magnitude greater than the calculated 1/f noise in the tunnel junctions. The factors contributing to the long term drift of the SQUID are discussed. By regulating the temperature of the helium bath we have achieved a drift rate of $2\text{x}10^{-5}\phi_o\text{h}^{-1}$ over a 20h period. A detailed description is given of the coupling efficiency of various input coils wound on the SQUID. The effects of coupling between the input coil, the SQUID, and the feedback (modulation) coil are described, and measurements of the coupling parameters reported. The energy resolution of the SQUID with respect to a current in a 24-turn input coil is $7\text{x}10^{-30}\text{JHz}^{-1}$ for frequencies at which the flux noise has a white power spectrum. In terms of energy resolution, the SQUID has a better performance in the 1/f noise region than that of any SQULD previously reported in the literature. The long term drift over an extended period also represents the lowest value yet reported.

1. INTRODUCTION

Quantum interference effects in a superconducting ring containing two Josephson junctions[1] were first observed in 1964 by Jaklevic et al.[2] using tunnel junctions. These workers showed that the critical current of the double junction was an oscillatory function of the magnetic flux threading the ring, the period being the flux quantum, ϕ_o. The implications of this work in the measurement of magnetic fields and voltages were quickly realized and a number of dc SQUIDs (Superconducting Quantum Interference Devices) were soon developed and exploited. These devices included several designs involving point contact junctions[3-5], and the SLUG[6] (Superconducting Low-inductance Undulatory Galvanometer). Of these devices, the dc SQUID of Forgacs and Warnick[5] had the most highly developed readout electronics. Subsequently, the rf SQUID was developed.[7-9] This device incorporates a single junction in a superconducting ring, and presumably because only a single junction is required, has become much more widely used than the dc SQUID. Several commercial versions of the rf SQUID are available, and sophisticated readout electronics have been developed. The inherent noise in the rf SQUID has been studied in great detail[10], and close attention has been paid to the optimum coupling of the SQUID to the room temperature electronics. As a result of these developments, the present rf SQUIDs, pumped at typically 30 MHz, are more sensitive than the first generation of dc SQUIDs. However, there is no intrinsic reason why a 30 MHz rf SQUID should be more sensitive than a dc SQUID. In fact, as we shall see, the dc SQUID can have a better performance than an rf SQUID

of comparable self-inductance pumped at 30MHz. The resolution of the early dc SQUIDs appears to have been limited by the unsatisfactory matching of the low impedance (~1 to 10Ω) junctions at liquid helium temperatures to the room temperature electronics. Even when a room temperature matching transformer was used, the overall noise temperature of the preamplifier was frequently well above room temperature, whereas the optimized noise temperature is about 1K.[11]

In this paper we describe the theory, fabrication, operation, and performance of a dc SQUID that makes use of two shunted[12] Nb-NbOx-Pb tunnel junctions.[13] These junctions have predictable characteristics, can be stored for long periods at room temperature, and cycled between room and liquid helium temperatures repeatedly. The large area and capacitance of the junctions makes them very resistant to destruction by accidental electrical discharges. The devices can be operated at any temperature below about 6K because the temperature dependence of the critical current is relatively weak. The SQUIDs have a cylindrical geometry with an area of about $7mm^2$ and an inductance of about 10^{-9}H. We show a noise power spectrum for a typical SQUID. At frequencies above 2×10^{-2}Hz the noise is white with an rms flux noise of about $3.5\times10^{-5}\phi_o Hz^{-\frac{1}{2}}$, corresponding to a magnetic field noise of $10^{-10}G(Hz^{-\frac{1}{2}})$. At lower frequencies the flux noise power spectrum is approximately $10^{-10}(1Hz/f)\phi_o^2 Hz^{-1}$. However, as will be emphasized in the paper, the concept of flux noise is not very useful for comparing SQUIDs. A much more meaningful parameter is the energy per unit bandwidth associated with the minimum current change per $\sqrt{Hz}$ that can be detected in a coil coupled to the SQUID.[14]

For the SQUID described here, this parameter has a value of 7×10^{-30} JHz^{-1}. The average long term drift is $2\times10^{-5}\phi_o h^{-1}$. The energy resolution is significantly better than has previously been reported for dc SQUIDs, and is also better than that of most rf SQUIDS. The 1/f noise and long-term drift are lower than any values previously reported. The improvement in sensitivity over earlier dc SQUIDs results from the use of the superconducting resonant circuit to couple the SQUID to the preamplifier. Our electronics has a dynamic range in a 1Hz bandwidth of approximately $\pm3\times10^{6}$. A slewing rate of $2\times10^{4}\phi_o s^{-1}$ and a frequency response of several kHz are typical.

In Section 2 we describe the theory* of operation of the dc SQUID. We have adopted a simple model that yields results in agreement with our measured parameters to within a factor of 2. (A detailed discussion of dc SQUID behavior, including the effects of noise, will be published subsequently.) We also describe the interaction of the SQUID with the tank circuit. Section 3 contains the details of the SQUID fabrication and mounting, and of the cryostat. In Section 4 we describe the essential features of the electronics associated with the SQUID, and the way in which the system is operated. The slewing rate, frequency response, and dynamic range are discussed. Section 5 is concerned with noise and drift. We discuss the noise contributions of the SQUID itself (Johnson noise and 1/f noise), and of the preamplifier, and compare these estimates with measured noise power spectra. The factors involved in obtaining good

---

* Good semi-quantitative descriptions of the dc SQUID have been given by De Waele and Ouboter[15] and Tinkham [16].

long term drift characteristics are discussed at length. In Section 6 we describe the proper noise characterization of the SQUID and the coupling of coils to the SQUID. Because these two topics are intimately connected, it is appropriate to discuss them together. After a discussion of the noise characterization, we briefly review the model circuit due to Webb, Giffard, and Wheatley[17] that demonstrates the importance of the intercoupling of the SQUID, the input coil, and the feedback coil. We then present measurements of all of the relevant SQUID and coil inductances and mutual inductances. From the noise and inductance measurements we calculate a figure of merit for the SQUID. Section 7 contains a summary and suggestions for possible improvements.

Preliminary brief reports of this work have appeared elsewhere.[18]

2. THEORY OF OPERATION

2.1 The Basic SQUID

The dc SQUID consists of two Josephson junctions on a superconducting ring of inductance L (Fig. 1). When the magnetic flux ϕ threading the ring is steadily changed, the total critical current, I_c, of the two junctions oscillates with a period of one flux quantum, ϕ_o.

In principle, any kind of Josephson junction may be used in a SQUID. In our SQUIDs we use resistively shunted thin-film tunnel junctions. It is essential that the current-voltage (I-V) characteristic of the SQUID be non-hysteretic, and a brief summary of hysteresis in tunnel junctions is in order. The theory of resistively shunted tunnel junctions was given

by Stewart[19] and McCumber[20], and has been experimentally verified by Hansma et al.[12] We assume that the current flows uniformly through the junction which is shunted by a capacitance C and a resistance r, as indicated in Fig. 1. (Note: Throughout the paper we use the following convention: The parameters i, i_c, v, and r represent the current, critical current, voltage, and resistance of a single junction, while the parameters I, I_c, V, and R represent the same quantities for a double junction. Thus $I_c = 2i_c$, $R = r/2$, etc.) The i-v characteristic exhibits hysteresis when the hysteresis parameter $\beta_c = 2\pi r^2 i_c C/\phi_o \gtrsim 1$, and no hysteresis when $\beta_c \lesssim 1$.[12,19,20] For our junctions, $i_c \sim 2\mu A$ and $C \sim 200pF$. To eliminate hysteresis, we resistively shunt each junction so that $r \lesssim 1\Omega$. Although the i-v characterisitc has been calculated[19,20] for the general case $C \neq 0$, for our purpose it is sufficient to use the result for $C = 0$. In this limit, the time-averaged voltage in the absence of noise is given by[19,20]

$$v = r(i^2 - i_c^2)^{\frac{1}{2}}, \quad (\beta_c = 0) \tag{2.1}$$

where $i \geq i_c$ is the bias current supplied to the junction. The dynamic resistance of the i-v characteristic is

$$r_D = (\partial v/\partial i)_{i_c} = r/[1 - (i_c/i)^2]^{\frac{1}{2}}. \tag{2.2}$$

The magnitude of the signal from the SQUID is a function of the modulation amplitude, $\Delta I_c = I_c[n\phi_o] - I_c[(n + \frac{1}{2})\phi_o]$, which, for two identical junctions, is determined solely by the parameter $\beta = LI_c/\phi_o$. As I_c is increased from 0 to ∞, ΔI_c increases smoothly from 0 to an asymtotic value of ϕ_o/L[3,6,15,21]. In practice, we choose $\beta \sim 1$ (see below), in which case it can be shown that

$$\Delta I_c \approx \phi_o/2L. \quad (\beta \sim 1) \tag{2.3}$$

For $L \approx 10^{-9}$H, $\Delta I_c \approx 1\mu$A.

When the critical current is reduced below its maximum value by the magnetic flux, the I-V characteristic is no longer given by Eq. (2.1). It is modified for low values of voltage, as sketched in Fig. 2. The modification of the I-V characteristic is produced by supercurrents flowing around the SQUID at the Josephson frequency (and higher harmonics[15]) associated with the dc bias voltage across the SQUID. As the voltage bias is increased from zero, the frequency of the ac currents increases. Once this frequency exceeds $2R_D/\pi L$, the amplitude of the circulating current is attenuated by the increasing ring impedance [$\sim (16R_D^2 + \omega^2L^2)^{\frac{1}{2}}$] and its effect on the I-V characteristic diminishes. Thus we expect the I-V characteristic to be strongly dependent on ΔI_c for $V < 2\phi_o R_D/\pi L$ and relatively independent of ΔI_c for $V > 2\phi_o R_D/\pi L$ as indicated in Fig. 2.

To observe the oscillations in critical current, the SQUID is biased

with a current I_o so that $0 < V < 2\phi_o R_D/\pi L$ for all values of net flux ϕ. The voltage across the SQUID is then also an oscillatory function of ϕ, with a modulation amplitude $\Delta V \sim R_D \Delta I_c \sim R_D \phi_o/2L$. For $R_D \approx 1\Omega$ and $L \approx 10^{-9}$H, $\Delta V \sim 1\mu V$.

The reason for choosing $\beta \sim 1$ is now apparent. For a given value of L, as I_c is increased ΔI_c increases relatively slowly to its maximum value of ϕ_o/L, while R must be decreased to keep $\beta_c \lesssim 1$. Thus as I_c is increased, the small increase in ΔI_c is more than offset by the larger decrease in R, so that ΔV and the available signal power tend to decrease. On the other hand, if I_c is reduced much below $\phi_o/L \sim 2\mu A$, the value of ΔI_c decreases somewhat, but more importantly, the noise rounding[22-25] of the I-V characteristic becomes substantial, and the signal is reduced. A reasonable compromise between these two extremes occurs with $\beta \sim 1$.

2.2 SQUID Readout

To read out the critical current of the SQUID an ac sinusoidal flux of frequency ν_o = 100kHz and amplitude $\phi_m \approx \phi_o/4$ is applied to the SQUID. As illustrated in Fig. 3(a), the ac voltage across the SQUID has a large component at $2\nu_o$ and no component at ν_o when the quasistatic flux ϕ_q in the SQUID is $(n + \frac{1}{2})\phi_o$. As ϕ_q is increased, the amplitude V_o of the ac signal across the SQUID at frequency ν_o increases (initially linearly), while the component at $2\nu_o$ decreases. When $\phi_q = (n + 3/4)\phi_o$ the component at ν_o will have its maximum amplitude $\Delta V/2$ [Fig. 3(b)]. As ϕ_q is further increased V_o decreases and becomes zero again at $(n + 1)\phi_o$. The component at ν_o reverses phase at $\phi_q = n\phi_o$ and $(n + \frac{1}{2})\phi_o$. Figure 3(c) shows the variation of V_o with

ϕ_q in the vicinity of $\phi_q = (n + \frac{1}{2})\phi_o$. Although the exact value of $(\partial V_o/\partial \phi_q)_{I_o}$ near $(n + \frac{1}{2})\phi_o$ will depend in detail on the shape of the V vs. ϕ_q curve, a reasonable estimate would be $\sim 2\Delta V/\phi_o$.

The ac signal developed across the SQUID is amplified and lock-in detected at frequency ν_o. One of the major difficulties in the past has apparently been the satisfactory matching of the dc SQUID to the room temperature electronics.[11] The FET preamplifier used in our electronics has an optimum noise temperature at 100kHz of about 1K at a source impedance of $\sim 65k\Omega$. We have achieved satisfactory impedance matching by means of a cooled LC circuit resonant at frequency ν_o (Fig. 4). The superconducting coil has an inductance $L_T \approx 200\mu H$. In addition to providing an optimum source impedance for the preamplifier the tank circuit filters out most of the $2\nu_o$ component of the SQUID signal.

The reference signal for the lock-in is derived from the same oscillator that supplies the modulation flux. In the usual flux-locked loop in which the SQUID is operated, the output of the lock-in is fed back as a flux that opposes the applied flux. The feedback maintains the total quasistatic flux in the SQUID close to either $(n + \frac{1}{2})\phi_o$ or $n\phi_o$, depending on the phase of the lock-in reference signal, provided that the dynamic range and maximum slewing rate are not exceeded. The ac voltage across the SQUID at frequency ν_o is thus also maintained close to zero.

The ac modulation technique together with the negative feedback minimizes certain sources of drift and 1/f noise: For example, changes in the critical current caused by changes in the bath temperature; drifts in the bias current; drifts in the thermal emf's in the cryostat leads; and 1/f noise in the preamplifier.

The tank circuit on resonance presents (ideally) zero impedance to the SQUID. Any ac signal across the SQUID at frequency ν_o that would have an amplitude V in the absence of the tank circuit generates an ac voltage $V_c \approx QV$ across the tank circuit, where $Q = \omega_o L_T/R_D$, provided that R_D is the dominant resistance in the tank circuit. Thus when $\phi_q = (n \pm \frac{1}{4})\phi_o$, we expect $V_c^{(max)} \approx QR_D\phi_o/4L \approx \omega_o L_T\phi_o/4L$. A detailed model calculation of $V_c^{(max)}$ is carried through in Appendix A. In the model it is assumed that the I-V characteristic is given by Eq. (2.1), and that the I_c vs. ϕ curve is a triangle pattern. For this model we show that when $\Delta I_c = \phi_o/2L$,

$$V_c^{(max)} = \frac{\omega_o L_T \phi_o}{4L}\left(\frac{I_m}{I_o} - \frac{\phi_o}{4LI_o}\right), \tag{2.4}$$

where I_m is the maximum value of I_c. For $L_T = 200\mu H$, $L = 1nH$, $I_o/I_m = 1.3$, and $I_m = 4\mu A$, we calculate $V_c^{(max)} \approx 40\mu V$.

In the flux-locked mode, the sensitivity of the SQUID is determined by the parameter $(\partial V_c/\partial\phi_q)_{I_o}$. For the model in Appendix A, we show that this quantity is related to $V_c^{(max)}$ by the equation

$$\left|\left(\frac{\partial V_c}{\partial \phi_q}\right)_{I_o}\right| = \frac{16}{\pi}\frac{V_c^{(max)}}{\phi_o}. \tag{2.5}$$

If $V_c^{(max)} = 40\mu V$, $(\partial V_c/\partial \phi_q)_{I_o} \approx 200\mu V \phi_o^{-1}$. In view of the non-ideal behavior of the I-V characteristic resulting from noise rounding[22-25] and self-induced steps,[26] and because of the deviation of the I_c vs. ϕ curve from the assumed triangular pattern, Eq. (2.4) may be in error by as much as a factor of 2. However, we expect Eq. (2.5) to be reasonably accurate under all conditions.

The optimum bias voltage for the SQUID in this circuit could in principle be calculated, but in practice is always found empirically by adjusting I_o to obtain the maximum signal from the tank circuit. Usually the optimum bias is $I_o/I_m \approx 1.3$. This value will be used in various estimates of SQUID parameters. The dynamic resistance [Eq. (2.3)] of the SQUID at this bias is about 1Ω, so that $Q \approx 125$. The impedance of the resonant circuit presented to the FET amplifier, $Q^2 R_D$, is about 15kΩ. The reason for this choice of impedance will emerge in Section 4.

3. SQUID FABRICATION AND EXPERIMENTAL DETAILS

3.1 SQUID Fabrication

The design of our SQUID is shown in Fig. 5. The substrate for the metal films is a fused quartz* tube 20mm long with an o.d. and i.d. of 3mm and 2mm respectively. The tube is cleaned with Labtone cleaner, rinsed with distilled water, and finally heated with a torch to burn off residual surface contamination.

---

*Manufactured by U. S. Fused Quartz Inc. The paramagnetic susceptibility at 4.2K is less than 5×10^{-9} esu cm^{-3}. We are indebted to Dr. D. E. Prober and Mr. A. D. Smith for making this measurement.

A band of Pb/In (In content 5 to 10% by weight) 10.7mm wide and 3000Å thick is evaporated around the circumference of the tube. A Pb/In alloy rather than pure lead is used because it is more resistant to corrosion and appears to have less tendency to grow whiskers that may short the tunnel junctions. The deposition of the Pb/In band is followed by the evaporation of a 250μm wide 750Å thick gold film that serves as the shunt for the two junctions. The gold has an underlay (~50Å thick) of chromium to improve its adherence to the quartz. Next, two 150μm wide 3000Å thick niobium films, separated by 1.2mm are dc sputtered at a rate of about 1000Å/min with a Sloan Model S-300 Sputtergun. Each niobium film makes a low resistance contact with the gold film and a superconducting contact with the Pb/In band. The niobium is thermally oxidized for 12 minutes in air at 130°C in a closed oven. About 80% of the SQUIDs made with this oxidation procedure have critical currents in the acceptable range of 1 to 5μA.

Immediately after oxidation, a 3000Å thick Pb/In "T" is deposited. The crossbar of the T overlaps both the niobium strips to form two tunnel junctions. The crossbar is 75μm wide, giving each junction an area of about 1.1×10^{-2} mm^2. The stem of the T is 250μm wide, and bisects the gold strip between the niobium films to form a shunt for each junction. Next, the 10.7mm wide Pb/In band is scribed with a razor blade midway between the niobium films, as shown. One electrode for the SQUID is made by pressing a small piece of indium onto the base of the Pb/In T, while the second electrode is similarly attached to the base of the Pb/In band

on the reverse side of the cylinder.

The entire sensor is then coated with a thin insulating layer of Duco cement, applied by submerging the sensor twice in a solution containing 5 parts (by volume) acetone to 1 part Duco cement. We have found this insulator to be extremely reliable, and to recycle well between room and helium temperatures. Finally a 3000Å thick Pb/In ground plane(not shown In Fig. 5) is evaporated over the front surface of the SQUID. The ground plane reduces flux leakage through the slit in the Pb/In band and minimizes the inductance of the various metal strips leading to the junctions. A 500Å overlay of silver is deposited on top of the ground plane to protect the Pb/In from oxidation. Occasionally the ground planes are electrically shorted to the underlying films. We have found that shorted ground planes can readily be removed without damaging the tunnel junctions by immersing the sensor in acetone. The sensor is then recoated with cement and a new ground plane is deposited. The SQUID is completed by pressing leads of #40 copper wire to the electrodes with additional pellets of indium.

Typical parameters for the sensor are as follows: Capacitance per junction 200pf; critical current per junction 0.5μA to 2.5μA; and resistance per shunt 1Ω. We estimate the free standing inductance of the cylindrical part of the SQUID to be 0.75nH. The additional (parasitic) inductance contributed by the niobium and Pb/In strips is difficult to estimate accurately because of the uncertainties in the thickness of the insulating layer between the strips and the superconducting ground plane.

With an assumed insulator thickness of ~10μm, we estimate the parasitic inductance to be about 0.5nH.

These SQUIDs have proved extremely long-lived, with respect to both storage at room temperature and to thermal cycling. However, they need to be handled with reasonable care. When they are removed from the liquid helium we have found it advisable to enclose the end of the cryostat in a plastic bag filled with helium gas to avoid the condensation of excessive water vapor that may damage the ground plane. The SQUID must be free of condensed water before it is recooled because thermal contraction of the ice may result in cracking of the Duco cement insulator. We have also, on occasion, inadvertently destroyed SQUIDs by scatching the films when putting on or taking off input coils. The SQUIDs are very robust electrically. Current or voltage transients have never noticeably damaged the junctions although they have induced trapped flux in the junctions making a readjustment of I_o necessary.

3.2 SQUID Mounting and Shielding

To measure the intrinsic noise of the SQUID it is essential to screen it adequately from environmental magnetic fields. We have achieved excellent shielding by mounting the SQUID inside a long cylindrical tube machined from a rod of lead, 50/50 tin-lead solder, or niobium, as shown in Fig. 6. The lead and solder rods were made by casting commercial grade material in a mold. The niobium was 99.85% pure. The length of the tube is about 76mm, the inner diameter is 6.4mm, and the wall thickness is about 1mm. The middle region of the tube is tapped as shown. Two support screws of either fiberglass or a superconductor

are used to hold the SQUID in place. A short length of delrin rod is mounted in each screw with a nylon insert. The ac modulation and feedback coil, typically 2 turns of 50μm diameter insulated niobium wire of inductance 10nH, is wound on one of these rods.

Input coils (not shown in Fig. 6) are wound on the outside of the SQUID in the following way. The coil is wound from 75μm diameter insulated niobium wire on a teflon rod whose diameter is about 50μm greater than the o.d. of the SQUID. The coil is then coated with Duco cement. When the cement is dry, the excess is removed with a razor blade, and the coil is carefully removed from the teflon rod and mounted on the SQUID. This procedure produces a coil that is tightly coupled to the SQUID. Each pair of wires from the SQUID, modulation and feedback coil, and input coil is twisted together and passed through a small hole in one of the screws. The screws are then gently tightened to hold the SQUID rigidly in place. This assembly has proved to have negligible microphonic noise when the magnetic field trapped in the shield is $\lesssim$ 1G.

The expected attenuation of an external magnetic field by our cylindrical shield is calculated in Appendix B. Experimentally we find that this attenuation is $\gtrsim 10^{11}$ for all directions of applied field when the shield is initially cooled in an axial field of ~10mG. The performance with superconducting support screws is not significantly better than with fiberglass screws. With a 2.8G axial field applied during cooldown the attenuation is only $\sim 10^{10}$. Ideally, the attenuation of externally applied fields should in no way depend on the amount of trapped

flux threading the cylinder. In practice, we suspect that flux lines pinned in the shield or the SQUID move in a reversible fashion when an external field is applied, thus varying the flux in the SQUID. (A similar mechanism may be involved with temperature dependent effects to be discussed in Section 5.4).

The superconducting shield in which the SQUID is mounted acts as a ground plane to reduce the inductance of the SQUID cylinder. It has a negligible effect on the parasitic inductance, because of the presence of the superconducting film overlaying the niobium and Pb/In strips. The cylinder inductance is reduced by a factor* of about $(1-\delta)$, where δ is the ratio of the cross sectional area of the SQUID to that of the superconducting shield. In our case, $\delta \approx 0.25$, so that the effective cylinder

---

*Consider a long solenoid of cross sectional area A mounted coaxially inside an infinitely long superconducting cylinder of cross sectional area A'. The inductance of the solenoid will be $L = NB_1A/Ic$ where B_1 is the field inside the solenoid, I is the current through the solenoid, and N is the number of windings. Let B_2 be the field in the region between the shield and the solenoid. From Ampère's law $B_1 + B_2 = 4\pi NI/\ell c$, where ℓ is the length of the solenoid. Since the total flux through the shield is constant, $B_1A = (A' - A)B_2$. Thus $B_1 = [1 - (A/A')]\,4\pi NI/\ell c$, and $L(\delta) = (1 - \delta)L(0)$, where $\delta = A/A'$, and $L(0) = 4\pi N^2A/c^2\ell$. This ground planing effect of the shield will reduce the inductance of the SQUID cylinder (which can be thought of as a single turn solenoid) as well as the inductance of any input coils wound around the sensor.

inductance is approximately 0.55nH. Unfortunately, it is not possible to measure the total SQUID inductance L directly. Throughout the paper, we shall take a value of L = 1nH as a reasonable estimate of the sum of the cylinder and parasitic inductances. This estimate is consistent with the fact that the critical current modulation depth, ΔI_c, is typically 1μA.

3.3 Cryostat

The SQUID shield and the tank circuit are rigidly mounted on a copper plate suspended by stainless steel tubes inside a vacuum can. The temperature of the SQUID can be elevated above the bath temperature by means of a non-inductively wound heater. The temperature is monitored with an Allen-Bradley carbon thermometer also mounted on the copper plate. With exchange gas in the can the time constant is about 1s. A solenoid wound on the outside of the vacuum can can be used to apply a magnetic field parallel to the axis of the shield. The vacuum can is cooled in a fiberglass He^4 dewar that requires no liquid nitrogen. Two concentric μ-metal shields around the cryostat are sometimes used to reduce the ambient field to less than 10mG.

For some measurements, the temperature of the SQUID is regulated at 4.2K. Regulation is achieved by controlling the pressure of the He^4 vapor in the dewar. The temperature of the SQUID is measured by the carbon thermometer in an ac bridge. The output of the bridge is used to regulate a valve through which the helium gas from the cryostat is vented. This

technique compensates for changes in temperature resulting both from atmospheric pressure fluctuations and from the decrease in hydrostatic pressure of the helium bath as the liquid evaporates. The regulator maintains a constant temperature to within ±50μK for the two-day hold time of the dewar.

4. SQUID AND ELECTRONICS OPERATION AND PERFORMANCE

4.1 SQUID Operation

The SQUID is brought into operation by making various adjustments to the SQUID electronics (Fig. 7) with the feedback loop open. First, the bias current, I_o, and the ac modulation level are varied until a 100kHz signal appears at the output of the tuned amplifier. Next, the tank circuit trimmer capacitor is adjusted to maximize this signal. (The tank circuit resonant frequency is independent of the SQUID parameters, and the adjustment needs to be made only once for a given tank circuit.) As the amplitude of the ac modulation flux, ϕ_m, is increased from zero, the amplitude of the signal varies roughly as $J_1(2\pi\phi_m/\phi_o)$, where J_1 is the first order Bessel function. The modulation level is set so that the output is near the first maximum, corresponding to $\phi_m \approx \phi_o/4$. It is not necessary to re-adjust the ac modulation level while using a given modulation coil. Finally, I_o is adjusted. For the ideal junction described in section 2, as I_o is increased from zero the output ac signal should be zero until $I_o > I_m - \Delta I_c$. The signal should then increase steadily, reach a maximum,

and decay monotonically back to zero. In practice, as I_o is increased past the first maximum, a series of maxima and minima is observed. These oscillations are probably the result of self-induced steps[26] on the I-V characteristic. Their presence does not seem to degrade the SQUID performance. The first maximum is always the largest, and the SQUID is operated at that point. When $I_m \lesssim 5\mu A$, the largest signal usually occurs when $I_o \approx 1.3 I_m$. The maximum is quite broad, and no degradation in SQUID performance occurs if I_o is as much as ±10% away from its optimum value. The maximum amplitude of the 100kHz signal available from the tank circuit is typically $V_c^{(max)} \approx 30\mu V$, about 75% of the value predicted by Eq. (2.4). In view of the uncertainties in the values of the various parameters and the approximations involved in the calculation, we consider the agreement between predicted and measured values of $V_c^{(max)}$ to be satisfactory.

When the various adjustments have been made, the feedback switch is closed to put the SQUID into a flux-locked loop. The SQUID is locked to either a maximum or a minimum of the I_c vs. ϕ curve, depending on the polarity of I_o. The flux resolution of the SQUID is independent of the choice of polarity.

4.2 Electronics Design and Performance

The SQUID electronics is shown in Fig. 7. The 100kHz output of the tank circuit is amplified in three stages. The first stage is a low noise FET preamplifier with a broadband gain of 10^2, and a voltage noise at 100kHz of typically $1.4 nV Hz^{-\frac{1}{2}}$. The second stage is a tuned amplifier with a

Q~3 and a gain of 10^2 at 100kHz. The ac signal from the SQUID is monitored at the output of this amplifier. The final ac amplification is provided by a broadband amplifier with a gain that is adjustable between 0 and 300. The output of this stage is fed into a multiplier with a sine wave reference to demodulate the 100kHz component of the signal. The reference signal from the oscillator is shifted in phase by 90° to compensate for the phase lag between the tank circuit output and the modulating flux. The multiplier output contains components near zero frequency and near 200kHz. In addition there may be a small 100kHz signal arising from a dc offset at the input of the multiplier. The 100kHz and 200kHz components are filtered with LC traps. The filtered output is then integrated, as shown in Fig. 7. R_2 is the input-output leakage resistance of the operational amplifier ($\sim 10^{10}\Omega$). The zero frequency gain of the integrator is about 10^5. At frequencies above a few mHz the integrator gain g_I is

$$g_I = (1 + j\omega\tau_N)/j\omega\tau_I, \qquad (4.1)$$

where $\tau_I = 2R_1C_I$ is the effective integrator time-constant, and $\tau_N = R_NC_I$. The neutralization resistor R_N in series with C_I compensates for the roll-off in the frequency response of the tank circuit (see below).

When the feedback switch is closed the integrator output is connected to the feedback resistor R_f in series with the modulation and feedback coil. The modulation and feedback coil couples to the SQUID through the mutual inductance M_f. The feedback current seeks to null out changes in the applied flux. The voltage V_f across R_f is thus proportional to the applied flux. V_f is read out by means of a unity gain buffer amplifier having a 100Ω output impedance. V_f can be set to zero by applying the appropriate offset current to the modulation and feedback coil.

We now evaluate the performance of the electronics with regard to dynamic range, frequency response, and slewing rate with the SQUID in the flux-locked mode. The dynamic range of the flux-locked loop is the ratio of the maximum integrator output voltage $\pm V_f^{(max)}$ to the minimum detectable output signal voltage $V_f^{(min)}$. The optimum dynamic range is obtained by using the smallest value of R_f/M_f for which the noise contribution to V_f from the buffer amplifier is still small compared with the noise contribution from the SQUID. We usually choose R_f/M_f to be between $0.1V/\phi_o$ and $0.2V/\phi_o$, although we have occasionally used a value of $0.03V/\phi_o$. With $R_f/M_f = 0.03V/\phi_o$, noise from the buffer amplifier is just detectable. Our limit on V_f is ±10V, so that the maximum flux change that can be tracked with $R_f/M_f = 0.1V/\phi_o$ is $\pm 100\phi_o$. For a SQUID with a flux resolution per $\sqrt{Hz}$ of $S_\phi^{\frac{1}{2}}$ the smallest detectable flux in a bandwidth B is $S_\phi^{\frac{1}{2}} B^{\frac{1}{2}}$. For $S_\phi^{\frac{1}{2}} = 3.5 \times 10^{-5} \phi_o Hz^{-\frac{1}{2}}$ and B = 1Hz, the dynamic range is about $\pm 3 \times 10^6$. The upper limit on the dynamic range is set by the buffer amplifier at $\pm 10^7$.

The frequency response and slewing rate are determined by the total loop gain and by phase shifts introduced at the various stages of amplification. Giffard et al.[9] have analyzed the electronics for an rf SQUID where the only significant phase shift is that produced by the integrator. Davidson et al.[27] have analyzed the case of the voltmeter. In the case of our dc SQUID the phase shift produced by the tank circuit must be included in the analysis since the bandwidth, about 1kHz, is two orders of magnitude smaller than that of a typical 30MHz rf SQUID. The phase shift of the tank circuit is compensated by the neutralization circuit across the integrator. Thus our electronics is characterized by the following time constants: Tank circuit time constant $\tau_t = Q/\pi\nu_o$, neutralization time constant $\tau_N = R_N C_I$, and the effective integrator time constant τ_I. Additional time constants associated with the finite bandwidth of the tuned amplifier and the LC traps are relatively unimportant.

If ϕ_a is the flux applied to the SQUID at angular frequency ω, then the corresponding feedback flux ϕ_f will be

$$\phi_f = \frac{G(\omega)\phi_a}{1 + G(\omega)}, \quad (|\phi_a - \phi_f| \leq \frac{\phi_o}{2}) \tag{4.2}$$

where $G(\omega)$ is the total small-signal loop gain. At frequencies above a few Hz where the integrator gain is given by Eq. (4.1)

$$G(\omega) = \frac{g(1 + j\omega\tau_N)}{j\omega\tau_I(1 + j\omega\tau_t)}. \qquad (4.3)$$

Here g is the loop gain at $\omega = 0$, exclusive of the integrator, and is defined by

$$g = (\partial V_c/\partial\phi_q)_{I_o}\, g_a(\omega_o) g_m (d\phi_f/dV_f). \qquad (4.4)$$

In Eq. (4.4) $\phi_q = \phi_a - \phi_f$, $(\partial V_c/\partial\phi_q)_{I_o}$ is the forward transfer function [Eq. (2.5)], $g_a(\omega_o)$ is the ac gain at 100kHz from the preamplifier input to the multiplier input, and g_m is the multiplier gain, about 0.4. The quantity $(d\phi_f/dV_f)$ is the reverse transfer function given by

$$d\phi_f/dV_f = M_f/R_f. \qquad (4.5)$$

The frequency dependence of $|V_f|$ is given by

$$\left|\frac{V_f(\omega)}{V_f(0)}\right| = \left|\frac{G(\omega)}{1 + G(\omega)}\right| = \left\{1 + \frac{\omega^2\tau_I^2}{g^2(1+\omega^2\tau_N^2)}\left[1 + \omega^2\tau_t^2 - \frac{2g}{\tau_I}(\tau_t - \tau_N)\right]\right\}^{-1/2}. \qquad (4.6)$$

To ensure that ϕ_f does not cancel the 100kHz flux ϕ_m we require $|V_f(\omega_o)| \lesssim 2^{-\frac{1}{2}}|V_f(0)|$. At $\omega = \omega_o$, the ω^4 term in Eq. 4.6 dominates, leading to the constraint

$$\frac{\omega_o \tau_I \tau_t}{g\tau_N} \gtrsim 1. \quad (\omega_o\tau_t, \omega_o\tau_N \gg 1) \tag{4.7}$$

Equation (4.7) puts an upper bound on g for given τ_I, τ_t, τ_N. We expect g to be somewhat below this bound because phase shifts in the tuned amplifier and LC traps are no longer negligible at $\omega = \omega_o$.

At low frequencies $|V_f(\omega)/V_f(0)| = 1$. As the frequency is increased, $|V_f(\omega)/V_f(0)|$ exhibits a peak at $\omega = \omega_p$, and then falls to zero at higher frequencies. The angular frequency ω_p is given by

$$\omega_p^2 = \frac{1}{\tau_N^2}\left\{\left[1 + \frac{2g\tau_N^2(\tau_t - \tau_N)}{\tau_t^2\tau_I} - \left(\frac{\tau_N}{\tau_t}\right)^2\right]^{1/2} - 1\right\}. \tag{4.8}$$

In the limit $\tau_N \to 0$, $\omega_p = (g/\tau_I\tau_t)^{\frac{1}{2}}$, and $|V_f(\omega)/V_f(0)| = (\tau_t g/\tau_I)^{\frac{1}{2}}$. The neutralization circuit shifts ω_p to lower frequencies and reduces the amplitude of the peak. When $\tau_N \approx \tau_t$, $\omega_p = 0$ and the peak disappears. In practice we keep τ_N somewhat less than τ_t (by about a factor of two) so that excessive amounts of high frequency noise from the electronics will not be fed baek to the SQUID. Thus there is always a peak in $|V_f(\omega)/V_f(0)|$. In order to keep this peak small, and, at the same time to have a good frequency response, one needs τ_t to be short as possible. It is for this reason that we compromise and choose Q ~ 125 rather than

the value of 260 that would optimally match the SQUID to the preamplifier.

We have measured $|V_f(\omega)/V_f(0)|$ as a function of frequency for g = 584, $\tau_N = 1.78\times10^{-4}$s, $\tau_I = 2\times10^{-2}$s, and $\tau_t = 4.13\times10^{-4}$s. The measured curve is shown in Fig. 8 together with the response curve calculated from Eq. (4.6). The agreement is quite good, except that $|V_f(\omega)/V_f(0)|$ rolls off somewhat more rapidly than expected. The measured 3dB roll-off frequency occurs at 2kHz instead of the calculated value of 2.5kHz.

The slewing rate is the rate $\omega\phi_f$ at which the feedback flux changes. The maximum slewing rate occurs when the output voltage V_c from the tank circuit is a maximum: At low frequencies ($\omega\tau_N, \omega\tau_t \ll 1$) this maximum is $V_c^{(max)}$ [Eq. (2.4)]. Giffard et al.[9] have shown that for an ideal electronics design characterized by a single time constant $(d/dt)(\phi_f/\phi_o)_{max} \approx \pi^2\nu_o/8$. For our electronics, this result is modified to

$$\frac{d}{dt}\left(\frac{\phi_f}{\phi_o}\right)_{max} \approx \frac{\pi^2}{8}\frac{\tau_t}{\tau_N}\nu_o. \quad (\omega_o\tau_t, \omega_o\tau_N \gg 1) \tag{4.9}$$

With $\tau_t/\tau_N \approx 2$, we find $(d/dt)(\phi_f/\phi_o)_{max} \approx 2.6\times10^5\phi_o s^{-1}$. Our measured slewing rate is typically $2\times10^4\phi_o sec^{-1}$. This limit is set by the saturation of the multiplier for $V_c < V_c^{(max)}$. By varying the loop gain and the various time constants, we have achieved a slewing rate of $10^5\phi_o s^{-1}$, but at the cost of increased output noise. We believe this noise arises from the increased bandwidth of the closed loop that results in noise from the electronics being fed back into the SQUID.

5. NOISE AND DRIFT

In this section we shall describe the noise and drift limitations of the shielded dc SQUID in the absence of an input coil. We discuss first the white noise limitations due to intrinsic SQUID noise and preamplifier noise, and second, the intrinsic 1/f noise. We then show a typical noise power spectrum, and compare it with the predicted spectrum. Finally, we discuss in detail the factors contributing to the long-term drift in the output of the device.

To fully evaluate the performance of a SQUID, one must specify not only the rms flux noise as a function of frequency, but also the inductance of the SQUID and how well an input coil can be coupled to the sensor. A discussion of these additional factors will be deferred until section 6.

5.1 White Noise

There are two sources of white noise: Johnson noise in the shunt resistors, and preamplifier noise. We consider first the Johnson noise. No detailed analysis of the effect of Johnson noise on a dc SQUID has previously appeared in the literature. We shall therefore adapt models for the noise in single junctions to estimate the noise in a dc SQUID. Because of the complicated non-linear nature of a SQUID, it is possible that our calculation somewhat underestimates the true noise, but our results can at least be regarded as a lower limit.

Consider first a single shunted junction with $\beta_c = 0$. In the absence of noise the i-v characteristic is given by Eq. (2.1). In the presence of thermal noise in the shunt the i-v characteristic becomes rounded near $v = 0$. The degree of rounding increases as the parameter $\gamma = i_c\phi_o/\pi k_B T$ is decreased from ∞ ($T = 0$) to $0(i_c = 0)$. The shape of the noise-rounded i-v characteristic has been calculated by Ivanchenko and Zil'berman,[22] Ambegaokar and Halperin,[23] and Vystavkin et al.[24] The experiments of Falco et al.[25] are in good agreement with the calculations. Likharev and Semenov[28] have given an analytic expression for noise power spectrum for a shunted junction when $\gamma \gg 1$. For frequencies much less than the Josephson frequency at the voltage bias in question they find the noise current has a white power spectrum given by

$$s_i = \left[1 + \frac{1}{2}\left(\frac{i_c}{i_o}\right)^2\right]\frac{4k_B T}{r}. \qquad (5.1)$$

When the noise rounding is considerable, no analytic solution for the power spectrum exists. The numerical calculations of Vystavkin et al.[24] are presented graphically in Fig. 3 of their paper. For low values of normalized bias voltage $\bar{v} = v/i_c r$, it appears that the voltage noise power spectrum, s_v, is proportional to v. This result is consistent with an elegant and physical analysis by Fulton[29] who finds that $s_v = 2\phi_o\nu_J$ for low bias voltages, where $\nu_J = 2ev/h$. As $\bar{v}$ is increased, the noise increases to a maximum when $(\partial v/\partial i)_{i_c}$ is a maximum. At higher values of $\bar{v}$, Vystavkin et al.[24] find that the noise decreases again, and is apparently

quite close to the prediction of Likharev and Semenov.[28] Thus it appears that the Likharev-Semenov result is a good approximation for voltages at which the noise rounding is not too severe.

Each junction in the SQUID has a critical current of typically 2μA, corresponding to $\gamma \approx 25$ at 4K. If we assume Eq. (2.1) to be valid, the bias voltage for $r \approx 1\Omega$ and $i_o/i_c \approx 1.3$ is about 1.7μV, corresponding to $\bar{v} \approx 0.85$. An inspection of the i-v characteristics[22-25] for $\gamma \approx 25$ and $\bar{v} \approx 0.85$ indicates that it is not significantly different from the $\gamma \to \infty$ limit. In addition, Fig. 3 of the paper by Vystavkin et al.[24] shows that the noise power spectrum for* $\gamma \approx 25$ and $\bar{v} \approx 0.85$ is not very different from that for $\gamma = \infty$ and $\bar{v} = 0.85$ (it is very different for $\bar{v} \lesssim 0.4$). From these results we conclude that the Likharev-Semenov[28] analytic result is probably adequate for our SQUIDs. However, it could give a seriously incorrect result for bias voltages much less than $I_c R \approx 2\mu V$ or critical currents less than (say) 1μA. We shall use Eq. (5.1) to estimate the white noise of our SQUIDs.

The noise current per junction predicted by Eq. (5.1) will affect the double-junction SQUID in two independent ways: First, by inducing a voltage noise across the junctions and, second, by inducing a circulating current noise and hence a flux noise. The power spectrum B_V of the voltage noise referred to the input of the preamplifier has the form

*Note: Vystavkin et al.[24] use a parameter $\Gamma = 2\pi k_B T/i_c \phi_o$. For $i_c \approx 2\mu A$, and $T = 4.2K$, $\Gamma = 0.1$.

$$B_V = Q^2\left[1 + \frac{1}{2}\left(\frac{I_m}{I_o}\right)^2\right]\frac{4k_B T R_D^{\,2}}{R} \qquad (5.3)$$

for frequencies in the range $\nu_o(1-1/2Q) < \nu < \nu_o(1+1/2Q)$. The flux noise induced by the circulating current noise is uncorrelated with the voltage noise and has a spectrum B_ϕ given by

$$B_\phi = \left[1 + \frac{1}{2}\left(\frac{I_m}{I_o}\right)^2\right]\frac{k_B T L^2}{R} \,. \qquad (5.4)$$

We turn now to the preamplifier noise. At a frequency of 100kHz, the 1/f noise of the preamplifier is quite negligible. The noise of the FET input stage may be characterized* by a noise voltage source with a white power spectrum F_V and an independent noise current source with a white power spectrum F_C. The total voltage power spectrum $S^{(A)}$ referred to the input of the preamplifier is thus

$$S^{(A)} = F_V + F_C Q^4 R_D^{\,2}. \qquad (5.5)$$

The voltage noise dominates for $Q^4 R_D^{\,2} < F_V/F_C$ while the current noise dominates for $Q^4 R_D^{\,2} > F_V/F_C$. The two contributions are equal for $Q^4 R_D^{\,2} = F_V/F_C$. It is useful to compare Eq. (5.5) with the Johnson noise spectrum $S^{(J)} = 4k_B T R_D Q^2$ of a resistance R_D at 4.2K referred to the output

* For a discussion of the optimization of noise in amplifiers, see, for example, S. Letzter and N. Webster, IEEE Spectrum 7, 62 (1970).

of the tank circuit:

$$\frac{S^{(A)}}{S^{(J)}} = \frac{F_V + F_C Q^4 R_D^2}{4k_B T R_D Q^2}. \qquad (5.6)$$

The ratio $S^{(A)}/S^{(J)}$ is plotted as a function of Q in Fig. 9, for the values $F_V = 2\times10^{-18} V^2 Hz^{-1}$ and $F_C = 4\times10^{-28} A^2 Hz^{-1}$ that are typical for our preamplifiers, and $R_D = 1\Omega$. The ratio $S^{(A)}/S^{(J)}$ has a minimum value of about 0.25 at Q = 265. This implies a preamplifier noise temperature of about 1K.

However, as discussed in Section 4.2, it is preferable to use a somewhat smaller Q, typically 100 or 125. For these values of Q, F_V completely dominates $F_C Q^4 R_D^2$. If we take into account the voltage noise from the SQUID (Eq. 5.3), the total voltage noise power spectrum S_V referred to the input of the preamplifier is then given by

$$S_V = B_V + F_V. \qquad (5.7)$$

We now determine the flux resolution of the SQUID at frequencies $0 \leq \nu \leq \nu_o/2Q \approx 500Hz$. To obtain the flux resolution it is necessary to take into account the fact that flux applied to the SQUID is modulated at 100 kHz and that the output of the ac amplifier is demodulated with a multiplier. With the feedback loop open, the voltage noise and flux noise will produce a total mean square voltage $P_n(f)$ in a bandwidth df at some frequency $\nu = f$ $(0 \leq f \leq \nu_o/2Q)$ at the output of the multiplier. One defines the flux resolution per square root Hertz, $S_\phi^{\frac{1}{2}}$, as the <u>equivalent</u>

rms flux noise that must be applied to the SQUID to produce the same mean square voltage $P_n(f)$. When the SQUID is in a flux locked loop the action of the feedback circuit is to supply a <u>real</u> flux noise to the SQUID with a spectrum given by S_ϕ. In Appendix C we show that S_ϕ is related to S_V [Eq. (5.7)] and B_ϕ [Eq. (5.4)] through the expression

$$S_\phi = 2S_V\left(\frac{\partial V_c}{\partial \phi_q}\right)_{I_o}^{-2} + \frac{3}{2}B_\phi. \tag{5.8}$$

In the flux locked loop $(\partial V_c/\partial \phi_q)_{I_o}$ is given by Eq. (2.5). If we insert Eqs. (2.5), (5.3), (5.4), (5.7), and $Q = \omega_o L/R_D$ into Eq. (5.8) we find that

$$S_\phi = \frac{\pi^2\phi_o^2}{128(V_c^{max})^2}\left\{\frac{4k_BT\omega_o^2L_T^2}{R}\left[1 + \frac{1}{2}\left(\frac{I_m}{I_o}\right)^2\right] + F_V\right\} + \frac{3}{2}\left[1 + \frac{1}{2}\left(\frac{I_m}{I_o}\right)^2\right]\frac{k_BTL^2}{R}. \tag{5.9}$$

5.2. 1/f Noise in the SQUID

At some low frequency we expect the SQUID noise to become dominated by 1/f noise. As in the case of white noise, the 1/f noise will appear both as voltage noise and flux noise. The voltage noise component will be eliminated by the ac modulation technique, while the flux noise will not. We estimate the magnitude of this noise.

Clarke and Hawkins[30] studied the 1/f noise in single shunted tunnel junctions similar to those used in the SQUID. They found that the measured noise was quantitatively predicted by the thermal fluctuation model of Clarke and Voss[31]. According to this model equilibrium temperature fluctuations in the junction give rise to fluctuations in critical current, and thus to fluctuations in voltage when the junction is biased with a constant current i_o at a non-zero voltage. The power spectrum of the voltage fluctuations is predicted to be

$$s_v = \frac{k_B T^2 (\partial v/\partial i_c)^2_{i_o} (di_c/dT)^2}{[3 + 2\ln(w_1/w_2)]Cf}. \qquad (5.10)$$

In Eq. (5.10), w_1 and w_2 are the greater and smaller widths of the junction. C is the heat capacity defined by

$$C = w_1 w_2 [c_{Pb}\xi_{Pb} + c_{Nb}\xi_{Nb}], \qquad (5.11)$$

where ξ_{Pb} and ξ_{Nb} are the Ginzburg-Landau coherence lengths in lead and

niobium and c_{Pb} and c_{Nb} are the specific heats of lead and niobium at the temperature of the experiment. Inserting the values $w_1 = 150\mu m$, $w_2 = 75\mu m$, $c_{Nb} = 2.5\times10^{-3} J\,K^{-1}cm^{-3}$, $c_{Pb} = 8\times10^{-3} J\,K^{-1}cm^{-3}$, $\xi_{Nb} = 400\text{Å}$, and $\xi_{Pb} = 800\text{Å}$ at 4.2K, we find $C = 8.5\times10^{-12} J\,K^{-1}$. From Eq. (2.2), for $r \approx 1\Omega$ and $i_o/i_c \approx 1.3$ we find $(\partial v/\partial i_c)_{i_o} \approx 1.2\Omega$. For $i_c = 2.5\mu A$, at 4.2K we find typically that $(di_c/dT) \approx 1\mu AK^{-1}$. Inserting these values into Eq. (5.10) we find $s_v \approx 9\times10^{-24}(1Hz/f)V^2Hz^{-1}$.

The voltage noise of each of the two junctions in the SQUID will contribute independently to the flux noise. The flux noise power spectrum for the SQUID can therefore be written as

$$S_\phi = s_v L^2/2R_D^2. \tag{5.12}$$

Using the values $L \approx 10^{-9}H$ and $R_D \approx 1\Omega$, we find a mean square noise of about $10^{-12}(1Hz/f)\phi_o^2Hz^{-1}$. Noise rounding of the i-v characteristic will change the value of $(\partial v/\partial i_c)_{i_o}$ somewhat, but probably by no more than a factor of 2.

5.3. Measured Power Spectrum

In Fig. 10 we show the power spectrum, S_ϕ, of the noise of a shielded SQUID at 4.2K with no input coil. The power spectrum was taken by digitizing the signal from the output of the flux-locked system, and storing the digitized signal in a PDP-11/20 computer. A Fast Fourier Transform of this signal was taken, squared, and stored, and the process repeated, typically 30 times, to obtain an averaged power spectrum.

The noise of the SQUID is nearly white between 2×10^{-2}Hz and 200Hz with an rms value of about $3.5\times10^{-5}\phi_o Hz^{-\frac{1}{2}}$. The roll-off in the noise above 200Hz is a result of filtering in the electronics. Below 2×10^{-2}Hz the power spectrum is approximately 1/f, with a mean square value of about $10^{-10}(1Hz/f)\phi_o^2 Hz^{-1}$. At 4.2K, the maximum ac signal from the tank circuit, $V_c^{(max)}$, was about 30μV. When SQUIDs were cooled to 1.8K, the white noise was lowered somewhat, typically to $2\times10^{-5}\phi_o Hz^{-\frac{1}{2}}$. At the same time, the signal from the tank circuit increased by a factor of about 1.2.

If the SQUID and its shield were cooled in the presence of a magnetic field greater than about 1G we observed microphonic noise. The power spectrum at low fields was not significantly dependent on whether or not the bath temperature was regulated. Also, the noise was not noticeably different when the SQUID was in liquid helium rather than in the vacuum can.

The rms noise predicted by Eq. (5.9) with $V_c^{(max)} = 30\mu V$, $I_o/I_m = 1.3$, $L = 10^{-9}H$, $L_T = 200\mu H$, $T = 4.2K$, $R = 0.5\Omega$, and $F_V^{\frac{1}{2}} = 1.4nVHz^{-\frac{1}{2}}$ is $3.2\times10^{-5}\phi_o Hz^{-\frac{1}{2}}$. Given the uncertainties in the values of the parameters, the agreement with the measured noise is excellent.

At 1.8K the predicted rms flux noise is $2.0\times10^{-5}\phi_o Hz^{-\frac{1}{2}}$, a value which is somewhat closer to our measured noise then we can justify with our model. The fact that the

flux resolution of the SQUID improves as the temperature is lowered strongly suggests that the noise is domimated by intrinsic thermal noise in the SQUID.

The measured 1/f noise power spectrum is about two orders of magnitude higher than that predicted by Eq. (5.12). To check that the 1/f noise was not generated at the lock-in detector, we remeasured the noise power spectrum with several different values of gain in the ac amplifier. The measured noise did not change significantly when the gain was varied over a factor of ten, implying that the 1/f noise originated in the SQUID. In view of the rather large discrepancy between the observed and calculated values of 1/f noise we believe that this noise is not thermally generated in the junctions. The source is unknown, but we speculate that the motion of flux pinned in the thin films of the sensor could possibly contribute to the noise.

5.4 Drift

We found that the output of the flux-locked loop tended to drift over long periods of time (hours). Because a low drift is essential for some applications, we investigated the cause of the drift in some detail. Most of the drift was found to be associated with the temperature dependence of the signal from the SQUID. Although the mechanism of the temperature dependence is not completely understood, we have been able to characterize it in an empirical way through a number of experiments. As a result, we have been able to achieve a very low drift rate in our system.

We have resolved two contributions to the temperature sensitivity, $d\phi/dT$, of the SQUID output. One contribution is roughly proportional to the axial magnetic field trapped by the superconducting shield as it is cooled below its transition temperature. The sign of this contribution depends on the polarity of the axial field. The other contribution is nearly independent of magnetic field. The field dependent contribution dominates for fields $\gtrsim$ 0.2G.

Curve 1 of Fig. 11 shows the variation of $\phi_o^{-1} d\phi/dT$ with temperature for a SQUID with leads attached with indium contacts*. This curve was reproducible from day to day to about ±5% for a given SQUID/shield combination. The SQUID was mounted in a lead shield with lead support screws, and was cooled in an axial field of 2.85G. Two μ-metal cans around the cryostat reduced the transverse components of the earth's field to less than 10mG. The axial field was turned off once the shield was below its transition temperature. The temperature sensitivity has a sharp peak at about 3.4K produced by flux exclusion from the indium contacts. The peak is superimposed on a background value of $d\phi/dT$ that decreases with decreasing temperature. The fact that the background is decreasing rather than increasing with temperature indicates that it is not produced by paramagnetic impurities in the quartz substrate or in the delrin rod on which the modulation coil is wound.

*Our earliest SQUIDs had In-Bi alloy contacts. We found that at 4.2K $d\phi/dT$ was about 50 times greater than for SQUIDs with indium contacts. The transition temperature of the In-Bi was smeared over the range 3.4K to 6K. As the temperature was lowered flux was progressively expelled from the contacts giving rise to a temperature dependent flux through the SQUID.

The magnitude of $d\phi/dT$ is too large to be attributed to the temperature dependence of the superconducting penetration depths or to thermal contraction or expansion of the shield or SQUID. We suspect that the magnetic field-related temperature dependance arises from the reversible motion of flux lines pinned in the shield. To further investigate this hypothesis we measured $d\phi/dT$ as a function of temperature for a SQUID mounted in shields made of lead (with lead and fiberglass support screws), niobium(with niobium and fiberglass support screws), and 50/50 lead-tin solder (with solder support screws). The results are shown in Fig. 11, curves 2-6. The system was always cooled in an axial field of 2.85G. The same SQUID was used when taking all data for curves 2-6. However, a different SQUID and lead shield were in use when data points for curve 1 were taken. It seems reasonable to assume that the value of the trapped field will be comparable for open-ended cylinders (i.e., those with fiberglass support screws) of different materials. However, it is by no means clear that a cylinder with superconducting support screws will trap the same flux as the same cylinder with non-superconducting support screws. In the case of the lead cylinder, there seems to be no difference in the results obtained with superconducting and fiberglass support screws, whereas with the niobium cylinder $d\phi/dT$ was somewhat lower for fiberglass support screws than for niobium

support screws. The shapes of the curves for lead and niobium are very similar between 4.2K and 6K, although apparently there is a small drop in $d\phi/dT$ for Nb near 6.5K. For the solder cylinder $d\phi/dT$ was substantially higher than for the lead and niobium cylinders, and had a different temperature dependence. The relatively poor performance of the solder can probably be attributed to a very broad superconducting transition caused by inhomogeneities. The lowest dependence achieved was with the niobium cylinder with fiberglass support screws, for which $d\phi/dT \approx 0.6\phi_o K^{-1} G^{-1}$ at 4.2K.

The fact that $d\phi/dT$ is higher for solder and lead than for niobium imples that the effect is inherent in the solder and lead shields. In the case of the niobium shield, although we suspect the effect is still inherent in the shield, we have no certain way of establishing that we are not observing a contribution to $d\phi/dT$ that is intrinsic to the SQUID.

We also measured $d\phi/dT$ when the SQUID and its shield were cooled in ambient fields of 10mG or less. For a niobium shield, the expected value of $d\phi/dT$, based on the measurements in higher fields, is about $6\times10^{-3}\phi_o K^{-1}$. In fact, $d\phi/dT$ was found to be an order of magnitude higher, typically $0.05\phi_o K^{-1}$ to $0.1\phi_o K^{-1}$. We shall denote this residual field-independent component by $d\phi/dT|_o$. We found that $d\phi/dT|_o$ had no systematic temperature dependence, varied somewhat from SQUID to SQUID, and reversed sign when I_o was reversed. We suspected that the effect was related to an asymmetry in the SQUID. If the two junctions of the SQUID are not identical I_o will divide unequally between them, thereby linking flux to the SQUID.

If the critical currents change with temperature the flux generated by I_o will change, and produce a temperature-dependent drift. The sign of $d\phi/dT|_o$ will depend on the polarity of I_o. The fact that the SQUID is locked to a maximum or minimum of the I_c vs. ϕ curve implies that for a perfectly symmetric SQUID the SQUID output should not change when I_c is changed.

We have made estimates of $d\phi/dI_o$ on one SQUID by measuring the change in the output of a flux-locked SQUID when I_o was changed. We found $d\phi/dI_o \approx 0.007\phi_o\mu A^{-1}$ at 4.2K. This result imples that a stability of 1 part in 10^{-3} in I_o is sufficient to reduce the drift to below $10^{-5}\phi_o$. We were able to reduce $d\phi/dI_o$ significantly by controlling the distribution of I_o between the two junctions. The wire connected to the SQUID cylinder was removed and reattached to the lower end of one of the niobium strips. A third lead was attached to the end of the other niobium strip. The division of I_o between the two strips was controlled with a potentiometer. The output of the flux- locked SQUID varied with the potentiometer setting as I_o was redistributed around the Pb/In band. It was possible to find a setting for which the SQUID output was independent of I_o, i.e., for which I_o linked zero flux to the SQUID. This setting did not produce $d\phi/dT = 0$: In fact, the value of the residual $d\phi/dT$ did not depend strongly on the setting. This result is expected for non-identical junctions. Independently of the initial distribution of I_o, a change in temperature, and thus in the junction critical currents, will result in a redistribution of I_o, and an accompanying change in the flux linked to the SQUID by I_o.

Since it is possible to change both the sign and magnitude of the magnetic field-related component of $d\phi/dT$ one can cool down the SQUID and its shield in an appropriate field so that the magnetic field related $d\phi/dT$ cancels $d\phi/dT|_o$. There is then a limited temperature range over which the temperature dependence of the drift will be small. In practice, it is not difficult to obtain a net temperature dependence $\lesssim 5\times10^{-3}\phi_o K^{-1}$ over a range of 50mK.

From our measurements of $d\phi/dT$ we can estimate the expected long term drifts in the SQUID output resulting from decreases in the hydrostatic head presssure of the He^4 bath and variations in atmospheric pressure. In our fiberglass cryostat, the liquid helium level drops at a rate of no more than $25mmh^{-1}$ when the bath is at 4.2K. This drop results in a temperature decrease of up to $0.3mKh^{-1}$, and a corresponding magnetic field related drift of $\sim2\times10^{-4}\phi_o G^{-1}h^{-1}$. Atmospheric pressure related drifts, although typically comparable, may be a factor of five or more greater under extreme conditions. Thus for a SQUID and shield cooled in the earth's field, drifts of up to $5\times10^{-4}\phi_o h^{-1}$ are to be expected. To obtain low long term drift, one must either regulate the temperature of the SQUID or cool down the shield and SQUID in a magnetic field that minimizes $d\phi/dT$.

From a practical point of view it is inconvenient to cool the SQUID and its shield in exactly the right field to give a small net temperature dependence. As mentioned in section 3.3 we have constructed a simple temperature regulator that stabilizes the temperature to ±50μK. In Fig. 12 we show the drift over a 20h period of a temperature regulated

shielded SQUID whose temperature sensitivity was $0.1\phi_o K^{-1}$. The measurement bandwidth was OHz to 0.25Hz. The average drift is about $2x10^{-5}\phi_o h^{-1}$. We have also measured the drift in the output of a SQUID cooled in a magnetic field chosen to minimize $d\phi/dT$. Without temperature regulation the drift was again typically $2x10^{-5}\phi_o h^{-1}$.

The fact that the output of the flux-locked SQUID does drift despite all precautions suggests that yet another source of drift is present. The mechanism has been identified with a phase shift in the 100kHz signal produced by changes in the capacitance of the cable connecting the tank circuit with the preamplifier. The cable capacitance changes with temperature as the liquid He^4 level falls. In an ideal system in which the signal into the lock-in detector is maintained at a value close to zero by the feedback, this phase shift would not be important. However, because of the inductive coupling between the modulation coil and the SQUID, there is an unavoidable 100KHz feedthrough signal that is amplified by the tank circuit, and that is not reduced by the feedback. A change in the phase of this feedthrough will produce a change in the output of the lock-in. We found that a capacitance change of less than 1pF (0.01% of the tank circuit capacitance) could account for the drift observed over a 20h period. We hope to reduce the sensitivity to capacitance change in a future design of the electronics.

6. COIL COUPLING CONSIDERATIONS AND NOISE

6.1. Introduction

In most SQUID applications, the signal to be measured is coupled to the SQUID by means of a superconducting input coil. To make a voltmeter, the signal source and a calibrated resistor are connected in series with the coil. In the case of magnetometers, gradiometers, or susceptometers, the input coil is part of a superconducting flux transformer. Almost invariably the SQUID is used as a null detector by incorporating it into a negative feedback circuit. The feedback current can be coupled to these circuits in two ways. In most applications, it is highly desirable to use a "current nulling" technique wherein feedback is applied to the primary circuit rather than directly to the SQUID. For a voltmeter, the feedback current passes through the series resistor to maintain zero current in the circuit. This potentiometric technique has the obvious advantage of presenting a high input impedance to the signal source. Furthermore, calibration involves only a knowledge of the value of the series resistor. Extraneous circuit resistances and the mutual inductance between the input coil and the SQUID enter only in the loop gain of the feedback circuit. In the case of a flux transformer, the feedback current is coupled inductively to the transformer. This technique has the great advantage of introducing very little distortion into the field to be measured. In addition only a knowledge of the mutual inductance between the flux transformer and the feedback coil is required in the calibration. Stray circuit inductances and the mutual

inductance between the input coil and the SQUID affect the loop gain, but do not enter into the calibration of the flux sensitivity of the transformer.

In the alternative feedback mode which we shall refer to as "flux nulling" the flux applied to the SQUID by the input coil is canceled by an opposing flux generated by a feedback coil that couples directly to the SQUID. This method has the disadvantage of maintaining a non-zero current in the voltmeter circuit or flux transformer. One also needs to know the mutual inductance between the input circuit and the SQUID and the values of the extraneous resistances (for a voltmeter) or inductances (for a flux transformer) in order to calibrate the system. However, there are some measurements for which the flux nulling technique is essential.[9]

To properly characterize the sensitivity and noise of a SQUID in these applications, a knowledge of the flux noise power spectrum alone is not sufficient. One also needs to know how efficiently the signal to be measured can be coupled to the SQUID. This fact was recognized by Radhakrishnan and Newhouse[14], and has been discussed subsequently by other authors.[9, 11, 27, 32-34] A figure of merit that is appropriate for both magnetometers and voltmeters is the energy resolution per Hz referred to the input coil coupled to the SQUID.

A further parameter of interest is the mutual inductance M_{if} between the input and feedback coils; the possibility of such a coupling appears to have been neglected prior to the work of Webb, Giffard, and Wheatley.[17] Following their development, in the next section we consider a model circuit of a flux-locked SQUID coupled to a flux transformer, and discuss the influence of M_{if} on the behavior of the system. A method of measuring M_{if} is described. We show that M_{if} does not affect signal-to-noise considerations.

6.2. Model Circuit and Noise

Figure 13 shows a flux transformer with a pick-up loop of inductance L_p and an input coil of inductance L_i that is coupled to the SQUID via a mutual inductance $M_i = \alpha(LL_i)^{\frac{1}{2}}$. For simplicity, we neglect the stray inductance of the transformer, and assume that the pick-up coil has a single turn. The feedback coil of inductance L_f has a mutual inductance $M_f = \beta(LL_f)^{\frac{1}{2}}$ with the SQUID. Webb *et al.*[17] introduce a third mutual inductance M_{if} between L_i and L_f. $I_i(t)$ and $I_f(t)$ are the currents in the flux-transformer and the feedback coil. The negative feedback maintains the flux in the SQUID at a constant value.

Suppose a flux change $\Delta\phi$ is applied to L_p. In the flux transformer we have

$$\Delta\phi + (L_i + L_p)\, I_i + M_{if} I_f = 0. \qquad (6.1)$$

From the action of the feedback circuit we also have:

$$M_i I_i + M_f I_f + \phi_N = 0, \tag{6.2}$$

where $\phi_N(t)$ is the total effective flux noise of the SQUID. Eliminating I_f between Eqs. (6.1) and (6.2) we find

$$I_i = \frac{\phi_N(M_{if}/M_f) - \Delta\phi}{L_p + L_i(1 - M_{if}M_i/M_fL_i)}. \tag{6.3}$$

From Eq. (6.3) we deduce two results. First, a fraction of the flux noise of the SQUID is coupled into the flux transformer. Second, the <u>effective</u> inductance of the input coil is reduced to a value

$$L_i' = L_i\left(1 - \frac{M_{if}M_i}{M_fL_i}\right). \tag{6.4}$$

This is just the result obtained by Webb <u>et al.</u>[17] in their analysis of a voltmeter circuit. The effect of M_{if} is thus to increase the transformer current I_i generated by a given flux $\Delta\phi$.

We can also eliminate I_i between Eqs. (6.1) and (6.2) to find

$$I_f = \frac{[\Delta\phi M_i/(L_p + L_i)] - \phi_N}{M_f[1 - M_{if}M_i/(L_p + L_i)M_f]}. \tag{6.5}$$

From Eq. (6.5) we see that the presence of M_{if} is exactly equivalent to a reduction of M_f to an <u>effective</u> value

$$M_f' = M_f\left(1 - \frac{M_{if}M_i}{M_f(L_i+L_p)}\right). \tag{6.6}$$

In the limit $L_p = 0$, $M_f'/M_f = L_i'/L_i$. The effect of M_{if} is to increase the feedback current I_f required to oppose a flux change $\Delta\phi$ by a factor M_F/M_f'. In turn, the dynamic range and loop gain of the flux-locked SQUID are decreased by a factor M_f/M_f'. However, in priciple, it is possible to restore the dynamic range and loop gain to their original values by reducing the feedback resistor, R_F, to $R_F M_f'/M_f$. If $M_{if} > M_f(L_i + L_p)/M_i$, the phase of the feedback will be reversed, and the SQUID will lock-in at a maximum rather than a minimum in I_c, or vice versa. In this situation, the feedback is predominantly into the flux transformer rather than into the SQUID. If $M_{if} = M_f(L_i + L_p)/M_i$, the loop gain becomes zero.

The measurement of M_{if} is straightforward.[9] With the feedback loop <u>open</u>, one applies the appropriate current to the feedback coil to produce a flux change of exactly ϕ_o in the SQUID in each of two cases: (i) with L_i open, and (ii)with L_i superconductively shorted ($L_p = 0$). The required currents in the two cases are:

$$\Delta I_f^{(o)} = \phi_o/M_f, \quad (L_i \text{ open}) \tag{6.7}$$

and

$$\Delta I_f^{(s)} = \phi_o/M_f' = \Delta I_f^{(o)} \Big/ \left(1 - \frac{M_{if}M_i}{M_f L_i}\right), (L_i \text{ shorted}). \tag{6.8}$$

Thus if one measures the ratio $\Delta I_f^{(s)}/\Delta I_f^{(o)}$ and knows M_i, M_f, and L_i, one can immediately calculate M_{if}.

We can easily see from Eq. (6.5) that the flux resolution is independent of M_{if}. The smallest change in flux applied to the pick-up loop that can be resolved per $\sqrt{Hz}$ is just

$$\delta\phi = \frac{L_P + L_i}{M_i} S_\phi^{\frac{1}{2}} = \frac{L_p + L_i}{\alpha L^{\frac{1}{2}} L_i^{\frac{1}{2}}} S_\phi^{\frac{1}{2}}, \tag{6.9}$$

and is independent of M_{if}. The smallest value of $\delta\phi$ in a given pick-up loop that can be resolved is found by optimizing Eq. (6.9) with respect to L_i. We find that $\delta\phi$ has a minimum when $L_i = L_P$.[14,34] Thus

$$\delta\phi_{min} = 2L_P^{\frac{1}{2}} S_\phi^{\frac{1}{2}}/\alpha L^{\frac{1}{2}}. \tag{6.10}$$

The minimum detectable current per $\sqrt{Hz}$ in the input coil is $\Delta I_i = S_\phi^{\frac{1}{2}}/M_i$. The energy resolution per Hz, $L_i(\Delta I_i)^2/2$, is then

$$\frac{S_\phi}{2M_i^2/L_i} = \frac{S_\phi}{2\alpha^2 L}. \tag{6.11}$$

The quantity $S_\phi/2\alpha^2 L$ is an appropriate figure of merit for the SQUID/coil combination.

The smaller the value of $S_\phi/2\alpha^2 L$ the better is the performance of the SQUID/coil combination. One can readily measure L_i and M_i and thus estimate $\alpha^2 L$. It does not appear possible to measure separately α and L, whose values would be of some interest.

One other comment concerning the coupling of a SQUID to a flux transformer is appropriate here. If the SQUID is coupled to a superconducting circuit of total inductance L_ℓ via a mutual inductance M_i, Zimmerman[32] has pointed out that the effective SQUID inductance will be reduced to a value

$$L' = L\left(1 - \frac{M_i^2}{LL_\ell}\right). \qquad (6.12)$$

As a result, the signal available from the SQUID [Eq. (2.4)] will be enhanced by a factor $(1 - M_i^2/LL_\ell)^{-1}$. A corresponding improvement in the flux resolution and loop gain is to be expected. Now when the transformer is optimized, $L_\ell = 2L_i$ (ignoring stray inductances), and $M_i^2/L L_\ell = \alpha^2/2$. As we shall see in section 6.3, α^2 is at most 0.4, and the corresponding enhancement of the flux resolution is at most 20%. We have not felt it worthwhile to include this correction in the discussion of the optimization of the flux transformer.

We next describe the determination of L_i, M_i, $\alpha^2 L$, M_f, M_{if}, and L_i'.

6.3. Determination of L_i, M_i, $\alpha^2 L$, M_f, M_{if}, and L_i'

Our method of winding input coils is described in section 3.2. Four different coils were tested. The first was a relatively short coil (~1mm long) consisting of 8 closely spaced turns of 75μm diameter insulated niobium wire. The remaining three coils were all about 6mm in length, and consisted of 8, 16, and 24 turns respectively. To measure their inductance, each coil was connected in series with a resistor $R_i = 3.9\mu\Omega$. The leads between each coil and the resistor, typically 60mm long, were twisted, and had an inductance of about 20nH.* The free standing inductance of each coil L_c was calculated using standard formulas[35] and is shown in Table I. The coil was mounted in a lead shield together with a flux-locked SQUID, as shown in Fig. 14. The mutual inductance between the coil and the working SQUID was very small, typically 10^{-12}H or less, so that its inductance was not materially affected by the presence of the working SQUID. A sinusoidal current was applied to the coil circuit, and the output of the flux-locked SQUID measured as a function of frequency. The one-half power point was used to determine the inductance. We subtracted the estimated stray inductance, 20nH, from the measured inductance. The resulting shielded inductances, L_{sh}, are listed in column 3 of Table I, and are consistently lower than the calculated free standing inductances. This reduction is due to the ground-planing effect of the lead shield (see footnote on page 17). For each coil the ratio of the shielded inductance to the calculated inductance is listed

---

* Giffard et al.[9] have found that the self-inductance of a pair of tightly twisted superconducting leads is approximately 300nHm^{-1}.

in column 4 of Table I. As expected the value of this ratio for the long coils, 0.75, is close to $1-\delta$, where δ = coil area/shield area.

When the input coil is mounted on a SQUID, the inductance is further reduced by the ground-planing effect of the superconducting films. To estimate this effect, the coil was placed on an "open" SQUID in which the gold shunt and the Pb/In tee had been severed. Thus no currents circulated around the SQUID loop, but the ground-planing effect was comparable to that with a working SQUID. The measured inductances in this configuration minus 20nH are shown in column 5 of Table I. This shielded inductance is considerably lower than the free-standing inductance, and will be taken as the value of L_i. The total reduction in inductance in the presence of both the lead shield and the SQUID is higher for the short coil than for the long coil, as is seen from the ratio L_i/L_c shown in column 6 of Table I. It should be noted that L_i/L_c is essentially constant for the long coils.

The mutual inductance, M_i, of each coil with the SQUID was determined by measuring the current change required to produce a flux change ϕ_o in the SQUID with the feedback loop open. The values of M_i are shown in column 7 of Table I. The next column lists M_i divided by N, the number of turns on the coil. M_i/N is remarkably constant for all of the coils measured. Column 9 lists the values of $M_i^2/L_i = \alpha^2 L$. The values for the long coils increase slowly with the number of turns from 0.31nH for the 8-turn coil to 0.37nH for the 24-turn coil. As expected, $\alpha^2 L$ is smaller for the short 8-turn coil than for the long 8-turn coil. As

remarked previously, we cannot separately measure α and L. However, if we take our earlier estimate of L ≈ 1nH, then we find $\alpha^2 \approx 0.37$ for the 24-turn coil. It should be noted that the coil can couple flux only to the cylindrical inductance of the SQUID, and not to the stray inductance associated with the Pb/In and niobium strips. If we use our previous estimate of 0.55nH for the shielded inductance of the SQUID cylinder, then the coupling between the cylinder and the 24-turn coil is relatively good, with $\alpha^2 \approx 0.7$.

The values of L_i and M_{if} were determined for the short 8-turn coil and the long 24-turn coil. The 2-turn feedback coil used in these measurements had an inductance L_f of approximately 10nH. Its mutual inductance with the SQUID, M_f, was determined by measuring the current change $\Delta I_f^{(o)}$ required to produce a flux change ϕ_o in the SQUID with the input coil and the feedback loop open, and using Eq. (6.7). We found $M_f = 0.33$nH. The value in the absence of the input coil was not significantly different. We next measured $\Delta I_f^{(s)}$, the current change in the feedback coil required to produce a flux change ϕ_o in the SQUID with the input coil superconductivity shunted and the feedback loop open. We found $\Delta I_f^{(o)}/\Delta I_f^{(s)} = 0.5$ for the 8-turn short coil, and 0.12 for the 24-turn long coil. From Eqs. (6.4), (6.7), and (6.8), we find $\Delta I_f^{(o)}/\Delta I_f^{(s)} = L_i'/L_i = (1 - M_{if}M_i/M_fL_i)$. We thus immediately deduce L_i', and, knowing M_i, M_f, and L_i, calculate M_{if}. The values of L_i' and M_{if} are shown in the last two columns of Table I. For the 24-turn coil, the reduction in the effective inductance of the input coil is substantial.

The non-zero values of M_{if} have one other implication, namely that there will be coupling of the ac modulation flux to the input coil. For some applications it is important to reduce this coupling. Such coupling can be reduced significantly by means of a thin normal metal cylinder between the SQUID and the input coil. This cylinder will necessitate winding a signal coil with a slightly larger diameter, and will give rise to a somewhat lower value of $\alpha^2 L$.

6.4 Value of $S_\phi/2\alpha^2 L$

The value of $S_\phi/2\alpha^2 L$ for the SQUID whose noise spectrum is shown in Fig. 10 with the 24-turn coil is

$$\frac{S_\phi}{2\alpha^2 L} = 7 \times 10^{-30} \text{ J Hz}^{-1}. \qquad (6.13)$$

in the white noise region. The right hand ordinate of Fig. 10 has been labeled in units of J Hz^{-1}.

The short input coil and long input coils with fewer turns had smaller values of $\alpha^2 L$ and correspondingly larger values of $S_\phi/2\ \alpha^2 L$ For magnetometer and gradiometer applications the input coils tested had inductances of the appropriate order of magnitude. In voltage measuring applications somewhat higher values of L_i may be desirable. A factor of 10 could be easily achieved while keeping $\alpha^2 L \approx 0.4$ by winding a long, single layer, close-spaced input coil with the 75 μm diameter

niobium wire. L_i could be further increased by using a multiple layer input coil, although $\alpha^2 L$ would decrease somewhat due to the increased separation of the outer turns from the surface of the SQUID. To obtain $L_i > 3\mu H$ it would be advisable to go to a smaller wire size and retain the single layer configuration if possible.

7. DISCUSSION

We have used our SQUIDs in the laboratory as voltmeters. We have also used bare SQUID sensors in a three-axis magnetometer for geophysical exploration. We have found the design of our SQUIDs to be quite satisfactory, and no immediate changes in design are planned. The SQUIDs are very reliable with regard to thermal cycling and room temperature storage. Several SQUIDs were inadvertantly damaged in the process of mounting input coils. A small number of SQUIDs became inoperative after many thermal cyclings when the Duco cement layer cracked in the vicinity of the pressed indium contacts where the thickness was greater than elsewhere. Such SQUIDs could usually be repaired and used again. In the future, SQUIDs may be made entirely of niobium films using the Nb-Nb tunnel junctions recently developed.[36] Such SQUIDs should be more resistant to mechanical damage than the present SQUIDs.

We have shown that the white noise of our dc SQUIDs at 4.2K, typically $3.5 \times 10^{-5} \phi_o Hz^{-\frac{1}{2}}$, is close to the noise limit set by Johnson noise in the resistive shunts of the tunnel junctions. Although the noise theory needs further investigation, it is apparent that the only way to improve the

SQUID performance is to increase the resistance of the shunts. Because of the restriction on the hysteresis parameter ($\beta_c = 2\pi r^2 i_c C/\phi_o < 1$) an increase in r must be accompanied by a reduction in either i_c or C. However, because of noise rounding of the i-v characteristic it is undesirable to reduce i_c below its present value. Thus C alone can be decreased. This reduction can be achieved only by decreasing the area of the tunnel junction. Since $s_V^{\frac{1}{2}} \propto r^{-\frac{1}{2}} \propto C^{\frac{1}{4}}$ (for fixed β_c), an order of magnitude reduction in rms voltage noise would require a 4-order of magnitude reduction in junction area. The junction would then be of micron dimensions, a size that is attainable only by modern photoresist technology. However, a reduction in the volume of the junctions is expected to increase the 1/f noise of the junctions. In the present SQUIDs, the measured 1/f noise power spectrum was 2 orders of magnitude greater than that expected from the intrinsic 1/f noise in the junctions. Thus a 4-order-of magnitude reduction in the junction volume would be expected to increase the 1/f noise power spectrum of the SQUID by 2 orders of magnitude. It appears that a substantial reduction in the white noise can be achieved only at the expense of increased 1/f noise.

The long term drift of the SQUID output has been reduced to $2\times10^{-5}\phi_o h^{-1}$ by regulating the temperature of the helium bath. We believe that this residual drift results from the dependence on He^4 level of the capacitance of the leads connecting the tank circuit to the FET preamplifier. We hope to largely eliminate this source of drift in a future design of the electronics.

The energy resolution of our SQUID using a 24-turn input coil, $S_\phi/2\alpha^2 L$, is about 7×10^{-30} JHz^{-1}. It is of interest to compare this value with that of rf SQUIDs currently in use. The dc SQUID effectively generates and time-averages its own high frequency bias. At a typical bias voltage of 1μV, the Josephson frequency is about 500MHz. Thus one might expect the dc SQUID to have a comparable noise performance to an rf SQUID of the same inductance operated at 500MHz. T. D. Clark and L. D. Jackel[37] found for their 450MHz rf SQUID: $S_\phi = 9\times10^{-10}\phi_o^2$Hz^{-1}, $M_i = 3.5\times10^{-8}$H, and $L_i = 3\times10^{-5}$H. These values yield $S_\phi/2\alpha^2 L \approx 5\times10^{-29}$ JHz^{-1}. This energy resolution is about a factor of 7 poorer than that of our dc SQUID, which operates at a comparable frequency. We have also made measurements on two commercial* toroidal rf SQUIDs, operated at 19MHz and 30MHz. In each case, $S_\phi/2\alpha^2 L \approx 5\times10^{-29}$ JHz^{-1}, with an rf frequency about 20 times lower than the Josephson frequency of the dc SQUID. The best energy resolution that we are aware of was achieved by Pierce et al.[33] using a 10GHz rf SQUID. The resolution was 2×10^{-30} JHz^{-1} at frequencies above a few kHz; at lower frequencies the noise was appreciably higher.

*Manufactured by S.H.E. Corp., San Diego, California, and Superconducting Technology Inc., Mountain View, California, respectively.

8. ACKNOWLEDGEMENTS

We are indebted to Mr. T. D. Gamble for his help with the SQUID electronics. We have benefited greatly from many helpful and stimulating conversations with Professor R. P. Giffard. Professor Giffard also kindly read the manuscript and suggested numerous improvements. S.H.E. and S.C.T. collaborated with us in taking noise power spectra of their rf SQUIDs. This work was supported by the USERDA and the USGS. Part of the work was performed during the tenure of an IBM postdoctoral fellowship by W. M. G.

APPENDIX A. ESTIMATE OF TANK CIRCUIT OUTPUT AND FLUX SENSITIVITY FOR DC SQUID

We first calculate the amplitude V_c of the signal developed across the capacitor of the tank circuit in Fig. 4 when an ac flux at the resonant frequency is applied to the SQUID. Second, we calculate the quantity $(\partial V_c/\partial \phi_q)_{I_o}$ when the quasistatic flux ϕ_q is near $n\phi_o$ or $(n + \frac{1}{2})\phi_o$. We neglect the effects of noise rounding on the I-V characteristic, and assume that the I-V characteristic is of the Stuart-McCumber[19,20] form: $V = R(I_o^2 - I_c^2)^{\frac{1}{2}}$. (Here, I_c is a function of time through its dependence on the ac flux.) This form will be valid when $\beta \gg 1$, i.e. $\Delta I_c/I_c \ll 1$. We approximate the I_c vs. ϕ curve by a triangle pattern (Fig. 15) defined by

$$I_c = \begin{cases} I_m + 2\Delta I_c[(\phi/\phi_o) - (n+1)], & [(n+\frac{1}{2})\phi_o \leq \phi \leq (n+1)\phi_o] \\ I_m - 2\Delta I_c[(\phi/\phi_o) - n], & [n\phi_o \leq \phi \leq (n+\frac{1}{2})\phi_o]. \end{cases} \tag{A1}$$

Here, I_m is the maximum critical current, and ΔI_c is the modulation depth. We expect our model of a triangular I_c vs. ϕ curve to break down when $\Delta I_c \gtrsim 0.5 I_c$.

Because the tank circuit at resonance presents a low impedance to the SQUID, the SQUID is no longer current biased. If I_o is the dc bias current applied to the SQUID, we assume that $I_s(t)$ flows through the SQUID and that $I_o - I_s(t)$ is the current through the capacitor and coil (Fig. 4). By equating the voltage across the SQUID with that across the tank circuit, it is easy to show that the time dependent voltage $V_c(t)$ across the capacitor is the solution of the differential equation

$$- L_T C_T \ddot{V}_c + V_c = R[I_s^2 - I_c^2]^{\frac{1}{2}}, \qquad \text{(A2)}$$

where $I_s = I_o - C_T \dot{V}_c$. Eq. (A2) may be solved by squaring each side and substituting the Fourier series

$$V_c = \alpha_o + \sum_{n=1}^{\infty} \alpha_n e^{in\omega_o t} + \beta_n e^{-in\omega_o t}, \qquad \text{(A3)}$$

where $\omega_o = (L_T C_T)^{-\frac{1}{2}}$. If the flux in the SQUID is of the form $\phi = \phi_q + \phi_m \cos\omega_o t$ (ϕ_m is the amplitude of the modulation flux), then we may expand I_c^2 in a cosine series:

$$I_c^2(t) = \frac{a_o}{2} + \sum_{n=1}^{\infty} \frac{a_n}{2} (e^{in\omega_o t} + e^{-in\omega_o t}), \qquad \text{(A4)}$$

where

$$a_n = \frac{\omega_o}{\pi} \int_o^{2\pi/\omega_o} I_c^2(t) \cos n\omega_o t \, dt. \qquad \text{(A5)}$$

By solving for α_n and β_n in terms of a_n we find

$$V_c = - V_c \quad \sin\omega_o t \left[1 + O\left(\frac{R}{\omega_o L_T}\right)\right], \qquad \text{(A6)}$$

where $V_c = \omega_o L_T a_1 / 2I_o$. Since $R/\omega_o L_T \lesssim 10^{-2}$, the signal is almost perfectly sinusoidal and has an amplitude independent of R. It is important in designing a flux-locked

loop to realize that V_c is in quadrature with the ac modulation.

We must now evaluate a_1. From Eq. (A1), $I_c^2(t)$ is of the form

$$I_c^2(t) = \begin{cases} \left\{I_m + 2\Delta I_c\,[(\phi_q + \phi_m \cos\omega_o t)/\phi_o - (n+1)]\right\}^2, \\ \qquad [(n+\tfrac{1}{2})\phi_o \leq \phi_q + \phi_m \cos\omega_o t \leq (n+1)\phi_o] \\ \left\{I_m - 2\Delta I_c[(\phi_q + \phi_m \cos\omega_o t)/\phi_o - n]\right\}^2, \\ \qquad [n\phi_o \leq \phi_q + \phi_m \cos\omega_o t \leq (n+\tfrac{1}{2})\phi_o]\,. \end{cases} \tag{A7}$$

We restrict ourselves to values of ac flux such that $\phi_m < \phi_o/4$, so that the ac modulation sweeps over at most one cusp of the I_c vs. ϕ curve. There are then two distinct forms for a_1 depending on whether the ac flux sweeps over a maximum or minimum of I_c. Using Eqs. (A6) and (A7) we find for modulation about a minimum

$$a_1 = \frac{8\Delta I_c \phi_m}{\pi\phi_o}\left[\left(\frac{\phi_q - n\phi_o}{\phi_o}\right)\pi\Delta I_c + (I_m - \Delta I_c)\left(\gamma_n - \frac{\pi}{2} - \frac{\sin 2\gamma_n}{2}\right)\right], [n\phi_o \leq \phi \leq (n+1)\phi_o] \tag{A8}$$

where $\gamma_n = \cos^{-1}[(n\phi_o - \phi_q)/\phi_m]$. For modulation about a maximum we find

$$a_1 = \frac{8\Delta I_c \phi_m}{\pi\phi_o}\left[\left(\frac{\phi_q - (n+1)\phi_o}{\phi_o}\right)\pi\Delta I_c - I_m\left(\gamma_{n+1} - \frac{\pi}{2} - \frac{\sin 2\gamma_{n+1}}{2}\right)\right], \quad \left[(n+\tfrac{1}{2})\phi_o \leq \phi \leq (n+3/2)\phi_o\right]. \tag{A9}$$

The maximum amplitude $V_c^{(max)} = |V_c(t)|^{max}$ across the tank circuit occurs when $\phi_q \approx (n \pm \tfrac{1}{4})\phi_o$ and $\phi_m = \phi_o/4$. From Eqs. (A8) and (A9) we then find

$$a_1 = \pm \Delta I_c (I_m - \Delta I_c/2), \tag{A10}$$

the sign depending on whether $dI_c/d\phi_q$ is positive or negative. Inserting Eq. (A10) in Eq. (A6) we find

$$V_c^{(max)} = \frac{\omega_o L_T \Delta I_c}{2I_o} (I_m - \Delta I_c/2). \tag{A11}$$

To calculate the sensitivity of the SQUID in a flux-locked loop one needs to calculate $(\partial V_c/\partial \phi_q)_{I_o}$ near a maximum or minimum in I_c. From Eq. (A6) we have

$$\left(\frac{\partial V_c}{\partial \phi_q}\right)_{I_o} = \frac{\omega_o L_T}{2I_o} \frac{da_1}{d\phi_q}. \tag{A12}$$

Using Eq. (A8) one obtains

$$\frac{da_1}{d\phi_q} = \frac{16\Delta I_c}{\pi \phi_o} \left[\frac{\pi \Delta I_c \phi_m}{2\phi_o} + (I_m - \Delta I_c)\sin\gamma_n\right], \left[n\phi_o \leq \phi \leq (n+1)\phi_o\right] \tag{A13}$$

while from Eq. (A9) one obtains

$$\frac{da_1}{d\phi_q} = \frac{16\Delta I_c}{\pi \phi_o} \left[\frac{\pi \Delta I_c \phi_m}{2\phi_o} - I_m \sin\gamma_{n+1}\right], \left[(n+\tfrac{1}{2})\phi_o \leq \phi \leq (n+3/2)\phi_o\right]. \tag{A14}$$

At a minimum in I_c, $\gamma_n = \pi/2$ and

$$\left.\frac{da_1}{d\phi_q}\right|^{min} = \frac{16\Delta I_c}{\pi\phi_o}\left[\frac{\pi\Delta I_c \phi_m}{2\phi_o} + I_m - \Delta I_c\right], \tag{A15}$$

while at a maximum in I_c, $\gamma_{n+1} = \pi/2$ and

$$\left.\frac{da_1}{d\phi_q}\right|^{max} = \frac{16\Delta I_c}{\pi\phi_o}\left[\frac{\pi\Delta I_c \phi_m}{2\phi_o} - I_m\right]. \tag{A16}$$

The two expressions differ slightly because of the asymmetry introduced into the V vs. ϕ_q curve by the non-linearity of the I-V characteristic.

For the case $\phi_m = \phi_o/4$, we finally find

$$\left(\frac{\partial V_c}{\partial \phi_q}\right)_{I_o}^{min} = \left[\frac{8\omega_o L_T \Delta I_c}{\pi\phi_o I_o}\left(I_m - \frac{\pi\Delta I_c}{8}\right)\right], \tag{A17}$$

and

$$\left(\frac{\partial V_c}{\partial \phi_q}\right)_{I_o}^{max} = \left[-\frac{8\omega_o L_T \Delta I_c}{\pi\phi_o I_o}\left(I_m - (1 - \pi/8)\Delta I_c\right)\right]. \tag{A18}$$

From a practical point of view, it is useful to relate the maximum signal available from the tank circuit (at $\phi_q = (n\pm\frac{1}{4})\phi_o$) with the feedback loop open to $(\partial V_c/\partial\phi_q)_{I_o}$ near a maximum or minimum in I_c. Comparing Eq. (A11) with Eqs. (A17) and (A18) one finds

$$\frac{V_c^{(max)}/(\phi_o/4)}{(\partial V_c/\partial\phi_q)_{I_o}} = \frac{\pi}{4}\,\frac{(I_m - \Delta I_c/2)}{(I_m - K\Delta I_c)}, \tag{A19}$$

where

$$K = \begin{cases} \pi/8 \text{ near } \phi_q = n\phi_o \\ 1 - \pi/8 \text{ near } \phi_q = (n + \tfrac{1}{2})\phi_o . \end{cases} \tag{A20}$$

In our measurements, we find that the SQUID noise is not significantly different when the SQUID is locked at a maximum or minimum in I_c. In view of the various assumptions made in our calculation, the value of K may be a little unrealistic. It is therefore not unreasonable to replace K with its average value of 1/2. This assumption leads to the simple result

$$\left| \left(\frac{\partial V_c}{\partial \phi_q} \right)_{I_o} \right| = \frac{16\ V_c^{(max)}}{\pi\ \phi_o} . \tag{A21}$$

APPENDIX B. ATTENUATION OF MAGNETIC FIELD BY A HOLLOW SUPERCONDUCTING CYLINDER

The magnetic field inside an open-ended hollow superconducting cylinder of internal radius ρ_o and length $2z_o$ in the presence of an external field can be calculated as follows. The magnetic field is given by $\underset{\sim}{B} = -\nabla\Phi_m$, where Φ_m is the magnetic scalar potential. Φ_m can be expressed as [see Fig.16(a)]

$$\Phi_m(\rho,\phi,z) = \sum_{m=0}^{\infty}\sum_{n=0}^{\infty} J_m(K_{mn}\rho)[\sinh K_{mn}z(A_{mn}\sin m\phi + B_{mn}\cos m\phi) + \cosh K_{mn}z(C_{mn}\sin m\phi + D_{mn}\cos m\phi)] - B_o z. \qquad (B1)$$

Here, $K_{mn} = \gamma_{mn}/\rho_o$, where the γ_{mn} are the roots of $\partial[J_m(\rho)]/\partial\rho = 0$ ($\gamma_{00} = 3.83$, $\gamma_{10} = 1.84$, $\gamma_{20} = 3.05$). B_o is the field trapped when the cylinder becomes superconducting. If the magnetic fields in the planes $|z| = z_o$ are known, the coefficients A, B, C, D can be determined. The most penetrating magnetic field modes are those with m = 1, n = 0. The even J_1 mode couples to fields with components of $\partial B_z/\partial x$ or $\partial B_z/\partial y$ [Fig. 16(b)]. The odd J_1 mode couples to fields perpendicular to the axis of the cylinder [Fig. 1(c)]. At a distance of about 32mm from either end of the tube (i.e. at either end of the SQUID) the J_1 modes have been attenuated by a factor of 10^8. At the same position, the next most penetrating modes (m = 2, n = 0) are attenuated by a factor of over 10^{13}. The actual flux coupled to the SQUID by the field that does penetrate into the shield depends on the exact location of the SQUID. For both J_1 modes the coupling to a symmetrically located SQUID should be extremely weak: We estimate the attenuation to be as high as 10^{11}. The use of superconducting support screws may further attenuate externally applied fields.

APPENDIX C. FLUX RESOLUTION OF THE DC SQUID.

We calculate the flux resolution $S_\phi^{\frac{1}{2}}$ at low frequencies of a dc SQUID. The voltage noise power spectrum, due to both SQUID voltage noise and preamplifier voltage noise, is S_V [Eq. (5.7)], and the flux noise power spectrum is B_ϕ [Eq. (5.4)]. We consider the case where the flux applied to the SQUID is modulated by an ac flux $\phi_m \cos 2\pi\nu_o t$. The output of the SQUID is passed through a tank circuit that is resonant at ν_o and that has a bandwidth $2B = \nu_o/Q$. The signal from the tank circuit is amplified and then demodulated by a multiplier with a reference voltage that varies as $\sin 2\pi\nu_o t$. The multiplier output is filtered to remove frequency components near ν_o and $2\nu_o$, and thus only contains frequencies in the range $0 \leq \nu < B$.

Let $P_n(f)$ be the mean square voltage noise at a particular frequency $\nu = f$ in a bandwidth df at the output of the multiplier. One may write

$$P_n(f) = P_n^{(V)}(f) + P_n^{(\phi)}(f), \qquad \text{(C1)}$$

where $P_n^{(V)}(f)$ and $P_n^{(\phi)}(f)$ are the contributions from the voltage and flux noises. We have to calculate the value of the equivalent mean square flux $S_\phi df$ that must be applied to the SQUID in a bandwidth df to produce a mean square voltage P(f) at the output of the multipiier equal to $P_n(f)$.

The time dependent voltage noise $v_n(t)$ at the preamplifier input leading to $P_n^{(V)}(f)$ at the multiplier output contains frequency components in the two bands $\nu_o - (f + df) < \nu < \nu_o - f$ and $\nu_o + f < \nu < \nu_o + f + df$. For noise with a white spectrum we have

$$v_n(t) = \sum_{j=1}^{2} v_{nj}(t), \qquad (C2)$$

where

$$v_{nj} = \begin{cases} \alpha_1 \cos 2\pi(\nu_o - f)t + \beta_1 \sin 2\pi(\nu_o - f)t \\ \alpha_2 \cos 2\pi(\nu_o + f)t + \beta_2 \sin 2\pi(\nu_o + f)t. \end{cases}$$

Here, the α_j and β_j are the uncorrelated random amplitudes satisfying

$$\langle \alpha_j^2 \rangle = \langle \beta_j^2 \rangle = S_V df. \qquad (C3)$$

The voltage noise at the output of the multiplier after filtering is obtained by multiplying $v_n(t)$ by $g \sin 2\pi\nu_o t$ and dropping terms containing ν_o. The factor g is the total voltage gain after the tank circuit including that of the multiplier. From the definition of $P_n^{(V)}(t)$ we have

$$P_n^{(V)} = g^2 \left\langle \left(\sum_{j=1}^{2}{}' v_{nj}(t) \sin 2\pi\nu_o t \right)^2 \right\rangle, \qquad (C4)$$

$\sum'$ indicates that terms containing ν_o are to be dropped before squaring. Using Eq. (C3) with Eq. (C4) it is straightforward to show that

$$P_n^{(V)}(f) = \frac{1}{2} g^2 S_V df. \qquad (C5)$$

To calculate $P_n^{(\phi)}(f)$ we write the time dependent voltage across the tank circuit produced by the flux noise as

$$v_n^{(\phi)}(t) = (\partial V_c/\partial \phi_q)_{I_o} \phi_n(t) \sin 2\pi \nu_o t. \tag{C6}$$

Because of aliasing by the modulation flux in the SQUID we must consider frequency components of $\phi_n(t)$ near dc and near $2\nu_o$. We write

$$\phi_n(t) = \sum_{j=1}^{3} \phi_{nj}(t), \tag{C7}$$

where

$$\phi_{nj}(t) = \begin{cases} \gamma_1 \cos 2\pi f t + \delta_1 \sin 2\pi f t \\ \gamma_2 \cos 2\pi (2\nu_o - f)t + \delta_2 \sin 2\pi (2\nu_o - f)t \\ \gamma_3 \cos 2\pi (2\nu_o + f)t + \delta_3 \sin 2\pi (2\nu_o + f)t. \end{cases}$$

The γ_i and δ_i are uncorrelated, and satisfy

$$\langle \gamma_i^2 \rangle = \langle \delta_i^2 \rangle = B_\phi df. \tag{C8}$$

Combining Eqs. (C6) and (C7) one obtains

$$P_n^{(\phi)}(f) = g^2(\partial V_c/\partial\phi_q)^2_{I_o}\left\langle\left(\sum_{j=1}^{3\prime}\phi_{nj}\sin^2 2\pi\nu_o t\right)^2\right\rangle$$

$$= g^2(\partial V_c/\partial\phi_q)^2_{I_o} B_\phi df(\tfrac{1}{4} + \tfrac{1}{16} + \tfrac{1}{16})$$

$$= \tfrac{3}{8}g^2(\partial V_c/\partial\phi_q)^2_{I_o} B_\phi df. \qquad (C9)$$

The total mean square noise is given by adding Eqs. (C5) and (C9):

$$P_n(f) = \tfrac{1}{2}g^2 df[S_V + \tfrac{3}{4}(\partial V_c/\partial\phi_q)^2_{I_o} B_\phi]. \qquad (C10)$$

To obtain P(f) we assume that the equivalent flux applied to the SQUID has frequency components only near dc (i.e. none near ν_o or its harmonics). The calculation of P(f) otherwise follows the calculation of $P_n^{(\phi)}(f)$, and leads to

$$P(f) = \tfrac{1}{4}(\partial V_c/\partial\phi_q)^2_{I_o} g^2 S_\phi df. \qquad (C11)$$

If we compare Eq. (C11) with Eq. (C10) we find

$$S_\phi = 2S_V/(\partial V_c/\partial\phi_q)^2_{I_o} + 3B_\phi/2. \qquad (C12)$$

REFERENCES

1. B. D. Josephson, Phys. Lett. 1, 251 (1962); Adv. Phys. 14, 419 (1965).

2. R. C. Jaklevic, J. Lambe, A. H. Silver, and J. E. Mercereau, Phys. Rev. Lett. 12, 159 (1964).

3. J. E. Zimmerman and A. H. Silver, Phys. Rev. 141, 367 (1966).

4. M. R. Beasley and W. W. Webb, Proc. Symp. Physics of Superconducting Devices (Univ. of Virginia, Charlottesville, Apr. 28-29, 1967), V 1.

5. P. L. Forgacs and A. Warnick Rev. Sci. Instrum. 38, 214 (1967).

6. J. Clarke, Phil. Mag. 13, 115 (1966).

7. J. E. Zimmerman, P. Thiene, and J. T. Harding, J. Appl. Phys. 41, 1572 (1970).

8. J. E. Mercereau, Rev. Phys. Appl. 5, 13 (1970); M. Nisenoff, Rev. Phys. Appl. 5, 21 (1970).

9. R. P. Giffard, R. A. Webb, and J. C. Wheatley, J. Low Temp. Phys. 6, 533 (1972).

10. J. Kurkijärvi, Phys. Rev. B6, 832 (1972); J. Kurkijärvi and W. W. Webb in Proc. Appl. Superconductivity Conference, Annapolis (IEEE, New York, 1972), 581; J. Kurkijärvi, J. Appl. Phys. 44, 3729 (1973); L. D. Jackel and R. A. Buhrman, J. Low Temp. Phys. 19, 201 (1975).

11. J. Clarke, Proc. IEEE 61, 8 (1973).

12. P. K. Hansma , G. I. Rochlin and J. N. Sweet, Phys. Rev. 4B, 3003 (1971).

13. J. E. Nordman, J. Appl. Phys. 40, 2111-2115 (1969); J. E. Nordman and W. H. Keller, Phys. Lett. 36A, 52-53 (1971); L. O. Mullen and D. B. Sullivan, J. Appl. Phys. 40, 2115-2117 (1969); R. Graeffe and T. Wiik, J. Appl. Phys. 42, 2146-2147 (1971); K. Schwidtal, J. Appl. Phys. 43,

202-208 (1972);P. K. Hansma, J. Appl. Phys. 45, 1472-1473 (1974); S. Owen and J. E. Nordman, IEEE Trans. Magn. MAG-11, 774-777 (1975).

14. V. Radhakrishnan and V. L. Newhouse, J. Appl. Phys. 42, 129 (1971).
15. A. Th. A. M. De Waele and R. De Bruyn Ouboter, Physica 41, 225 (1969).
16. M. Tinkham, Introduction to Superconductivity (McGraw-Hill, 1975), 214.
17. R. A. Webb, R. P. Giffard, and J. C. Wheatley, J. Low Temp. Phys. 13, 383 (1973).
18. J. Clarke, W. M. Goubau, and M. B. Ketchen, IEEE Trans. Magn. MAG-11, 724 (1975); Appl. Phys. Lett. 27, 155 (1975); Proc. Fourteenth Intl. Conf. on Low Temp. Physics, (Helsinki, Finland, Aug. 14-20, 1975), 214.
19. W. C. Stewart, Appl. Phys. Lett. 12, 277 (1968).
20. D. E. McCumber, J. Appl. Phys. 39, 3113 (1968).
21. J. Clarke and J. L. Paterson, Appl. Phys. Lett. 19, 469 (1971).
22. Y. H. Ivanchenco and L. A. Zil'berman, Zh. Eksperim. I. Teor. Fiz. 55, 2395 (1968)[Sov. Phys. JETP 28, 1272 (1969)].
23. V. Ambegaokar and B.I.Halperin, Phys. Rev. Lett. 22, 1364 (1969).
24. A. N. Vystavkin, V. N. Gubankov, L. S. Kuzmin, K. K. Likharev, V. V. Migulin, and V. K. Semenov, Rev. Phys. Appl. 9, 79 (1974).
25. C. M. Falco, W. H. Parker, S. E. Trullinger, and P. K. Hansma, Phys. Rev. B10, 1865 (1974).
26. M. D. Fiske, Rev. Mod. Phys. 36. 221 (1964).
27. A. Davidson, R. S. Newbower, and M. R. Beasley, Rev. Sci. Instrum. 45, 838 (1974).

28. K. K. Likharev and V. K. Semenov, JETP Lett. 15, 442 (1972).

29. T. A. Fulton, IEEE Trans.Magn. MAG-11, 749 (1975).

30. J. Clarke and G. A. Hawkins, IEEE Trans. Magn. MAG-11, 724 (1975).

31. J. Clarke and R. F. Voss, Phys. Rev. Lett. 33, 24 (1974); R. F. Voss and J. Clarke, Phys. Rev. B 13, 556 (1976).

32. J. E. Zimmerman, J. Appl. Phys. 42, 4483 (1971).

33. J. M. Pierce, J. E. Opfer, and L. H. Rorden, IEEE Trans. Magn. MAG-10, 599 (1974).

34. J. H. Claassen, J. Appl. Phys. 46, 2268 (1975).

35. F. W. Grover, Inductance Calculations: Working Formulas and Tables (Dover Publications, Inc., 1962), 142-150.

36. Gilbert A. Hawkins and John Clarke, to be published in J. Appl. Phys.

37. T. D. Clark and L. D. Jackel, Rev. Sci. Instrum. 46, 1249 (1975).

TABLE I

Inductances and Mutual Inductance of Four Signal Coils. (L_c = calculated free standing inductance, L_{sh} = measured inductance of coil in lead shield minus 20nH. L_i = measured inductance of coil wound on open SQUID in lead shield minus 20nH.

Type of coil	L_c (nH)	L_{sh} (nH)	L_{sh}/L_c	L_i (nH)	L_i/L_c	M_i (nH)	M_i/N (nH)	M_i^2/L_i (nH)	L_i' (nH)	M_{if} (nH)
8-turn short	280	228	0.81	76	0.27	3.88	0.49	0.20	38	3.2
8-turn long	114	85	0.75	49	0.43	3.87	0.48	0.31		
16-turn long	380	290	0.75	168	0.44	7.61	0.48	0.34		
24-turn long	817	613	0.75	356	0.44	11.5	0.48	0.37	43	9.0

FIGURE CAPTIONS

Fig. 1 A tunnel junction dc SQUID. Each junction is modeled by an ideal Josephson junction (X) shunted by a resistor r and a capacitor C. A voltage V appears across the SQUID when it is biased with a current I greater than the critical current.

Fig. 2 Sketch of I-V characteristics of a dc SQUID with applied flux of $n\phi_o$ and $(n+\frac{1}{2})\phi_o$. When the flux is steadily changed, the voltage at a constant current bias I_o oscillates with a peak-to-peak amplitude of approximately $R_D\Delta I_c$, where R_D is the dynamic resistance.

Fig. 3 Output voltage of SQUID in response to an applied ac flux at frequency ν_o. In (a) the quasistatic flux $\phi_q = (n+\frac{1}{2})\phi_o$, and the output voltage is predominantly at $2\nu_o$. In (b) $\phi_q = (n+3/4)\phi_o$, and the output voltage is at ν_o. The amplitude, V_o, of the output voltage at ν_o as a function of ϕ_q is shown in (c).

Fig. 4 Schematic of SQUID showing the ac modulation coil and the resonant tank circuit used to read out the SQUID signal. At the resonant frequency (100kHz) the bias current I_o divides as shown. The output voltage V_c of the tank circuit appears across the capacitor C_T.

Fig. 5 Configuration of a thin film tunnel junction SQUID.

Fig. 6 SQUID mounted in superconducting shield.

Fig. 7 Schematic of the SQUID electronics. Components within the dashed box are at liquid He^4 temperature.

Fig. 8 Typical frequency response curve for a SQUID in a flux-locked loop. The solid line is calculated with no adjustable parameters, and the circles are measured data.

Fig. 9 Ratio of the preamplifier noise power $S^{(A)}$ to Johnson noise power in the SQUID shunts $S^{(J)}$ as a function of the tank circuit Q. The SQUID is optimally matched to the preamplifier when $Q \approx 265$.

Fig. 10 Typical noise power spectrum for a SQUID. The roll-off above 100 Hz is a result of electronic filtering, and is not intrinsic to the SQUID. The right hand axis specifies the energy resolution with respect to a 24-turn input coil.

Fig. 11 Temperature sensitivity $\phi_o^{-1} d\phi/dT$ vs. T for various types of SQUID shields and support screws.

Fig. 12 Long term output of a flux-locked SQUID with the temperature of the He^4 bath regulated at a nominal 4.2K. The measurement bandwith is dc to 0.25Hz.

Fig. 13 Model for the coupling between input coil L_i, feedback coil, L_f, and the SQUID. $I_i(t)$ and $I_f(t)$ are the input and feedback currents.

Fig. 14 Configuration for measuring the various self inductances and mutual inductances of coils.

Fig. 15 Model for the critical current of a SQUID as a function of net flux ϕ in the SQUID.

Fig. 16 (a) Hollow superconducting shield; (b) and (c) even and odd J_1 modes excited by external magnetic fields.

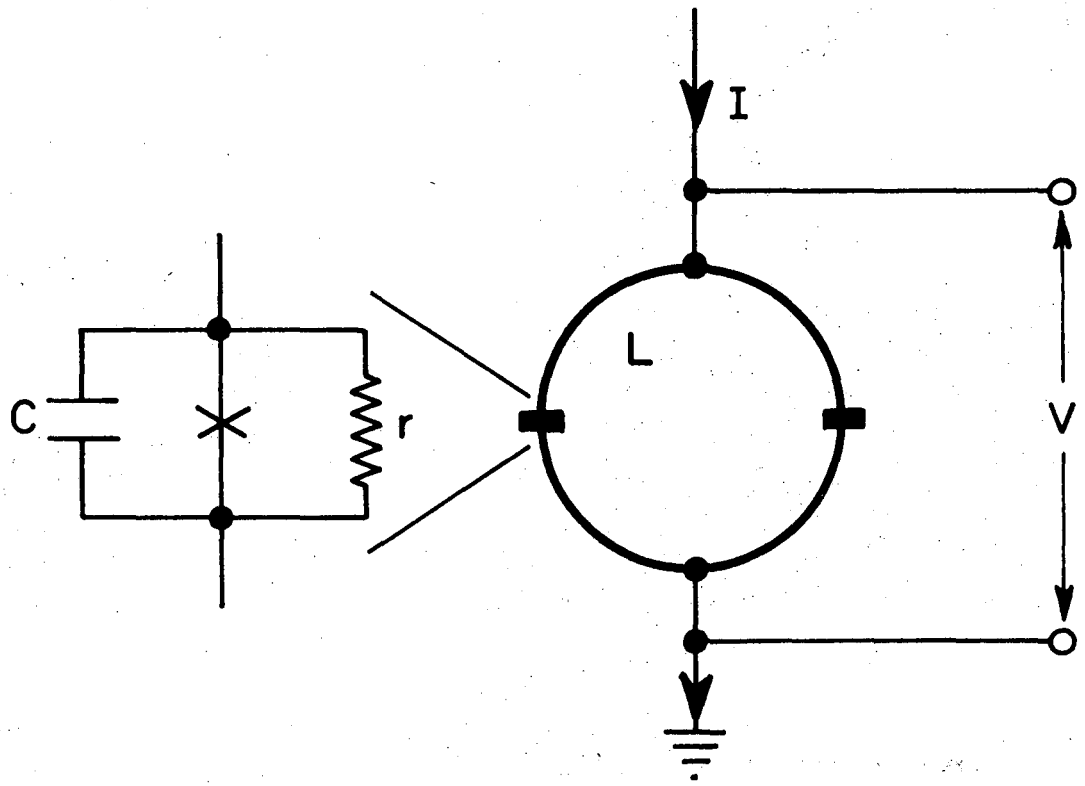

XBL 7511-9423

Fig. 1

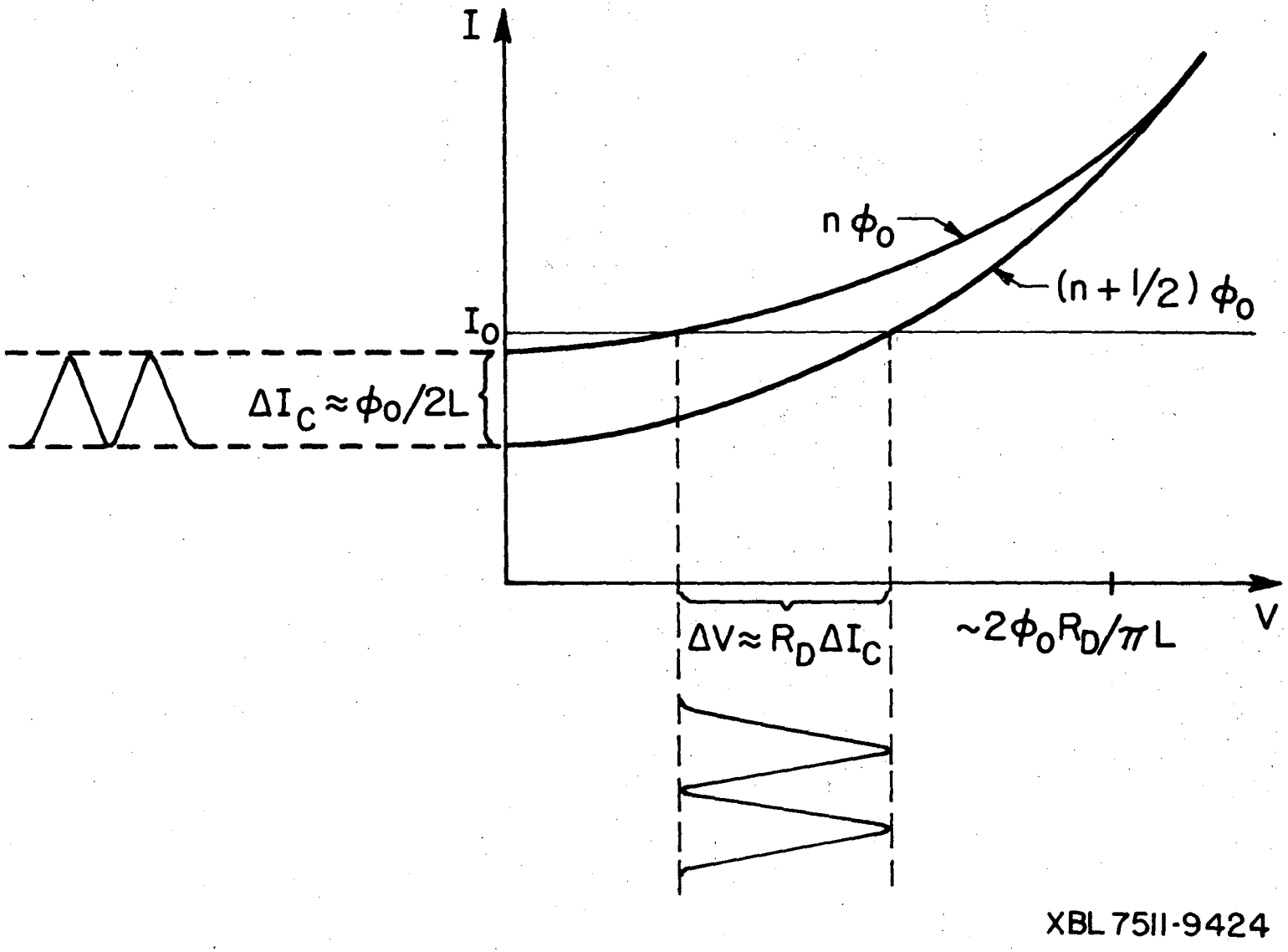
I
$n\phi_0$
$(n+1/2)\phi_0$
I_0
$\Delta I_c \approx \phi_0/2L$
$\Delta V \approx R_D \Delta I_c$
$\sim 2\phi_0 R_D/\pi L$
V
XBL 7511-9424

Fig. 2

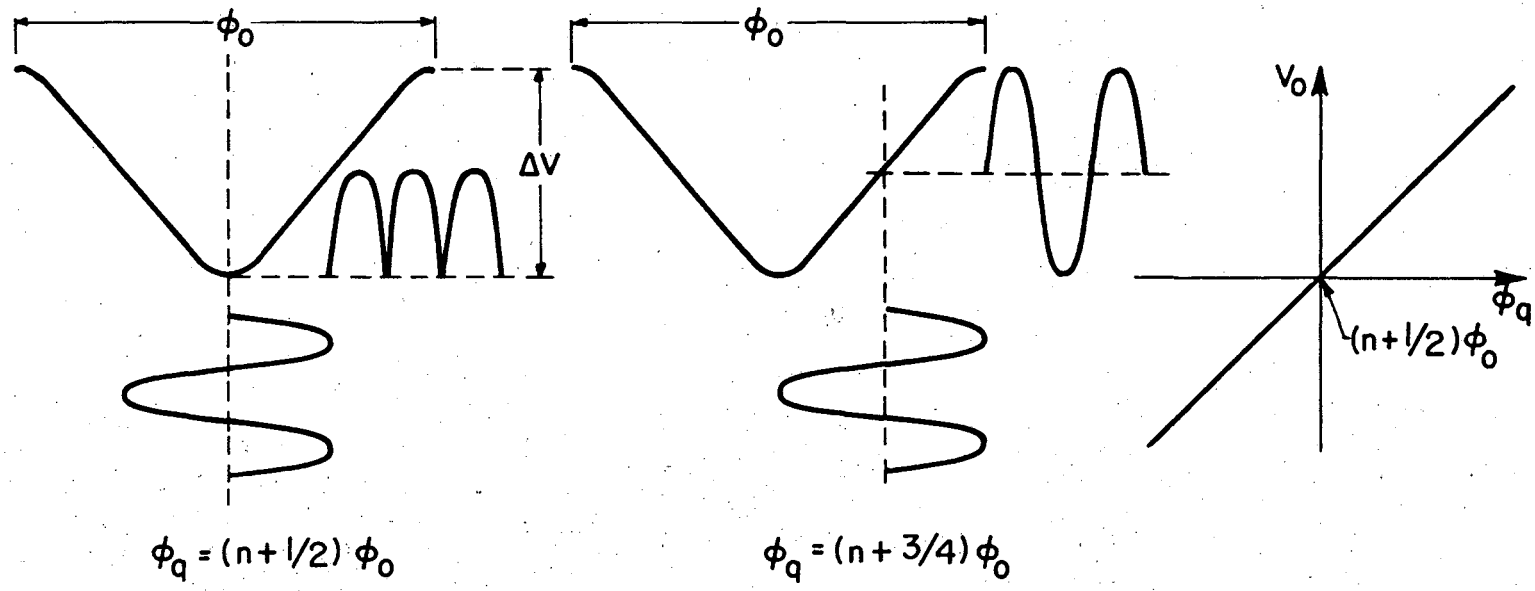

XBL7511-9425

Fig. 3

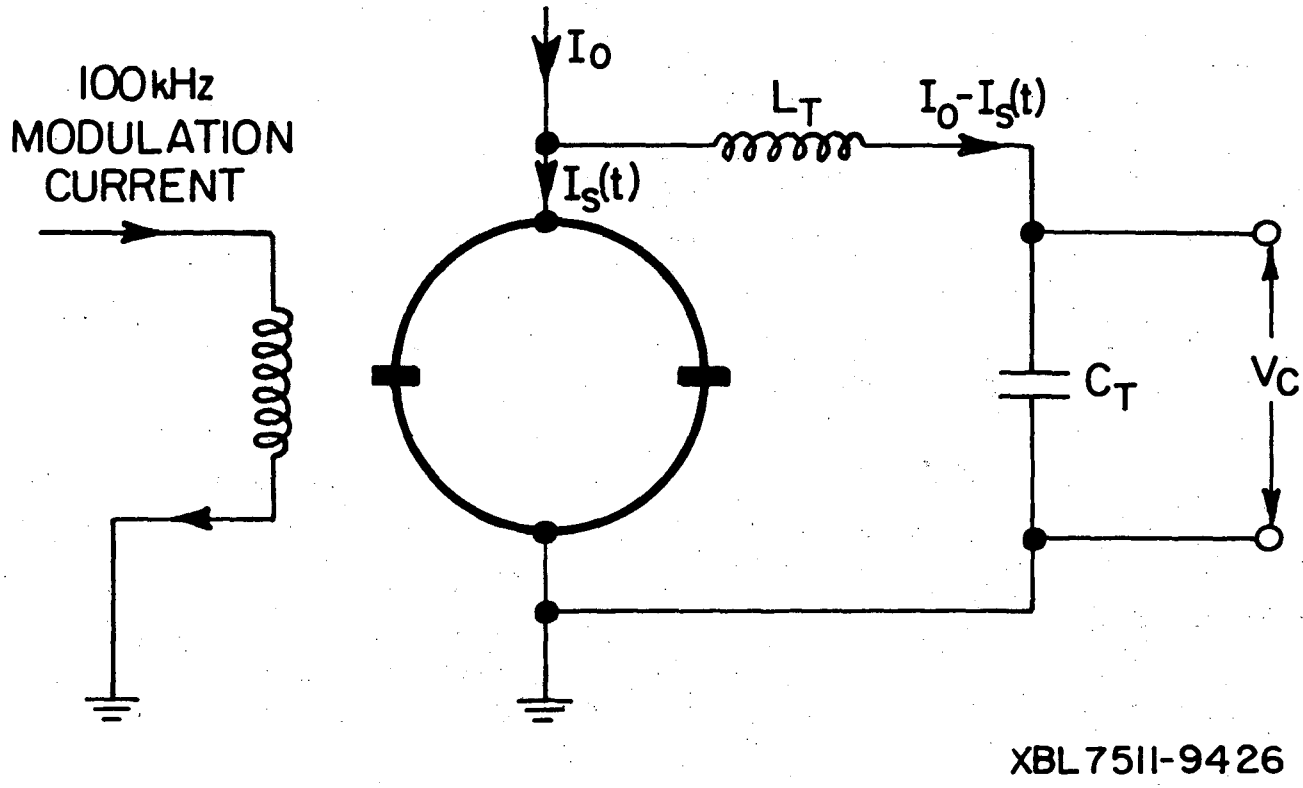
100kHz
MODULATION
CURRENT
I_0
L_T
$I_0-I_s(t)$
$I_s(t)$
C_T
V_C
XBL7511-9426

Fig. 4

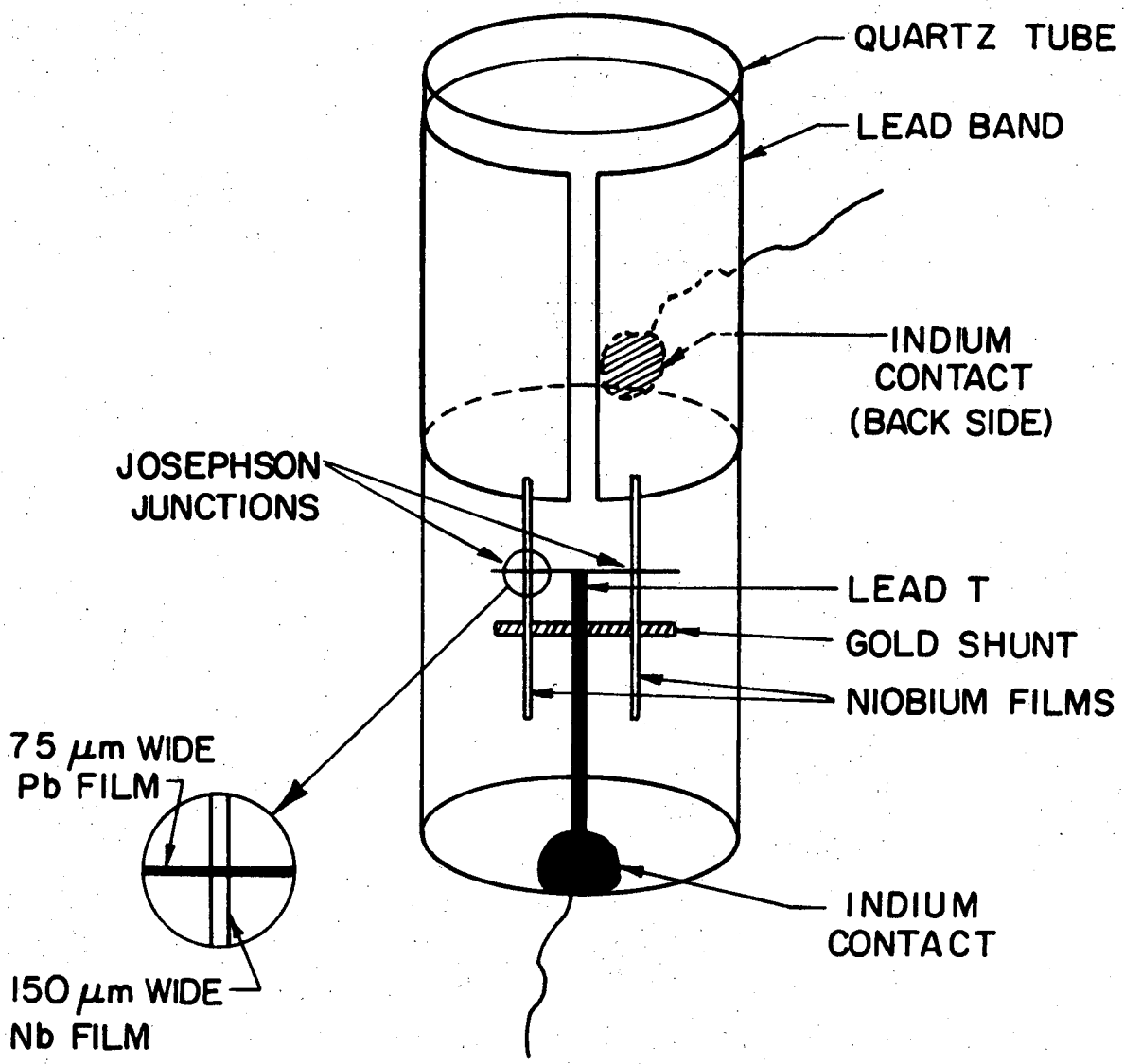

Fig. 5

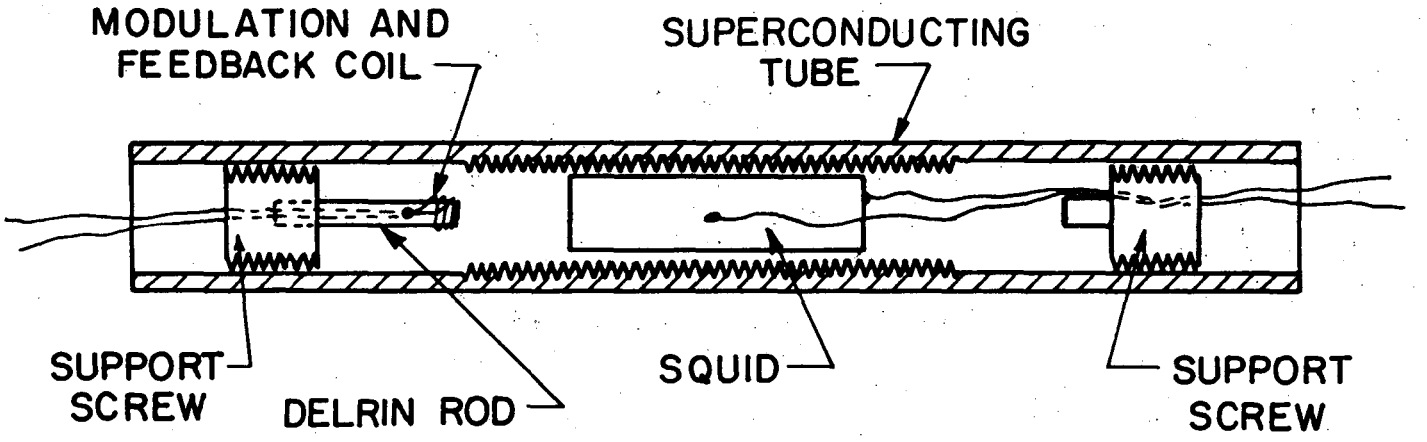
MODULATION AND
FEEDBACK COIL
SUPERCONDUCTING
TUBE
SUPPORT
SCREW
DELRIN ROD
SQUID
SUPPORT
SCREW
XBL749-7212A

Fig. 6

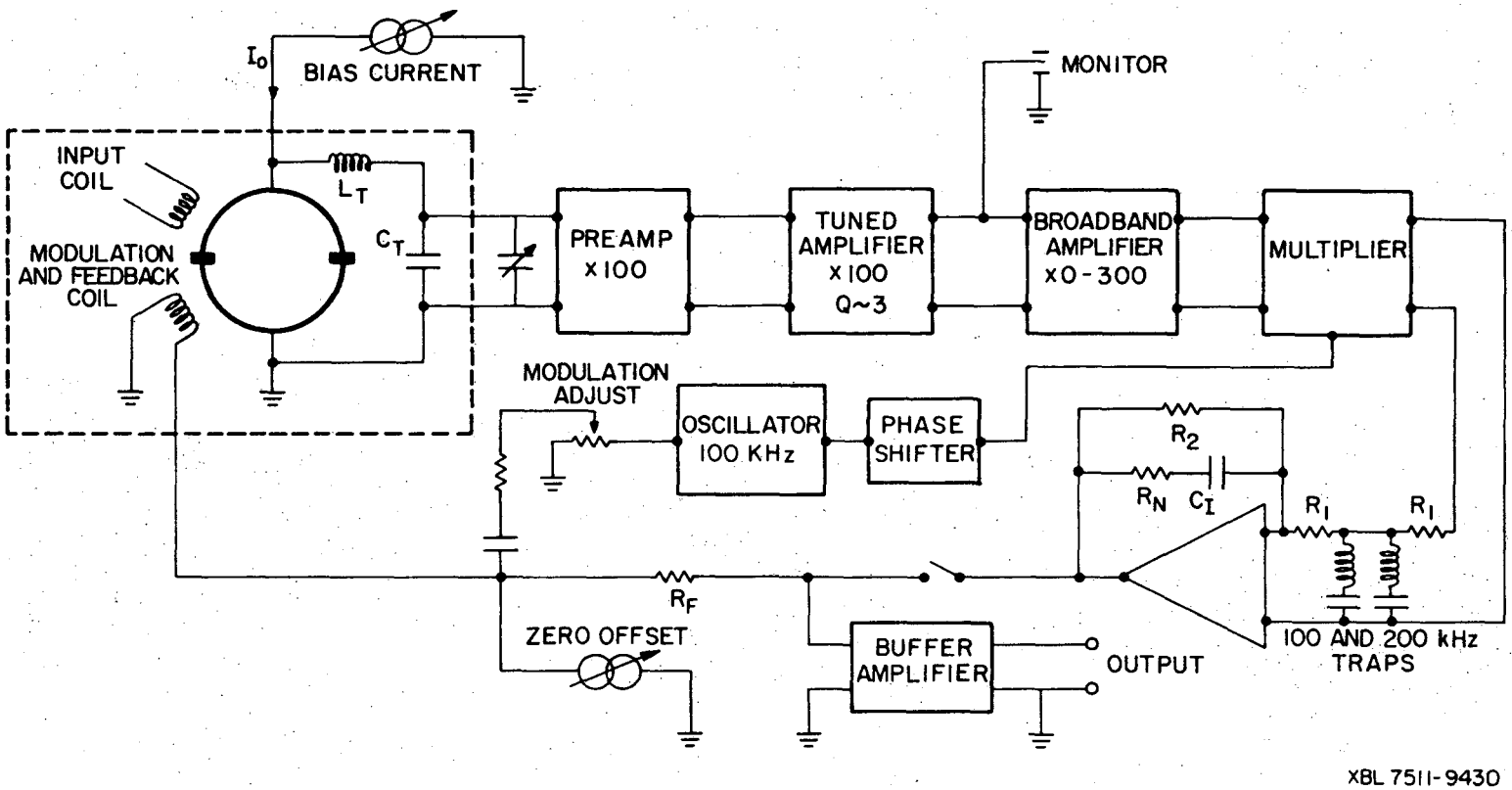

Fig. 7

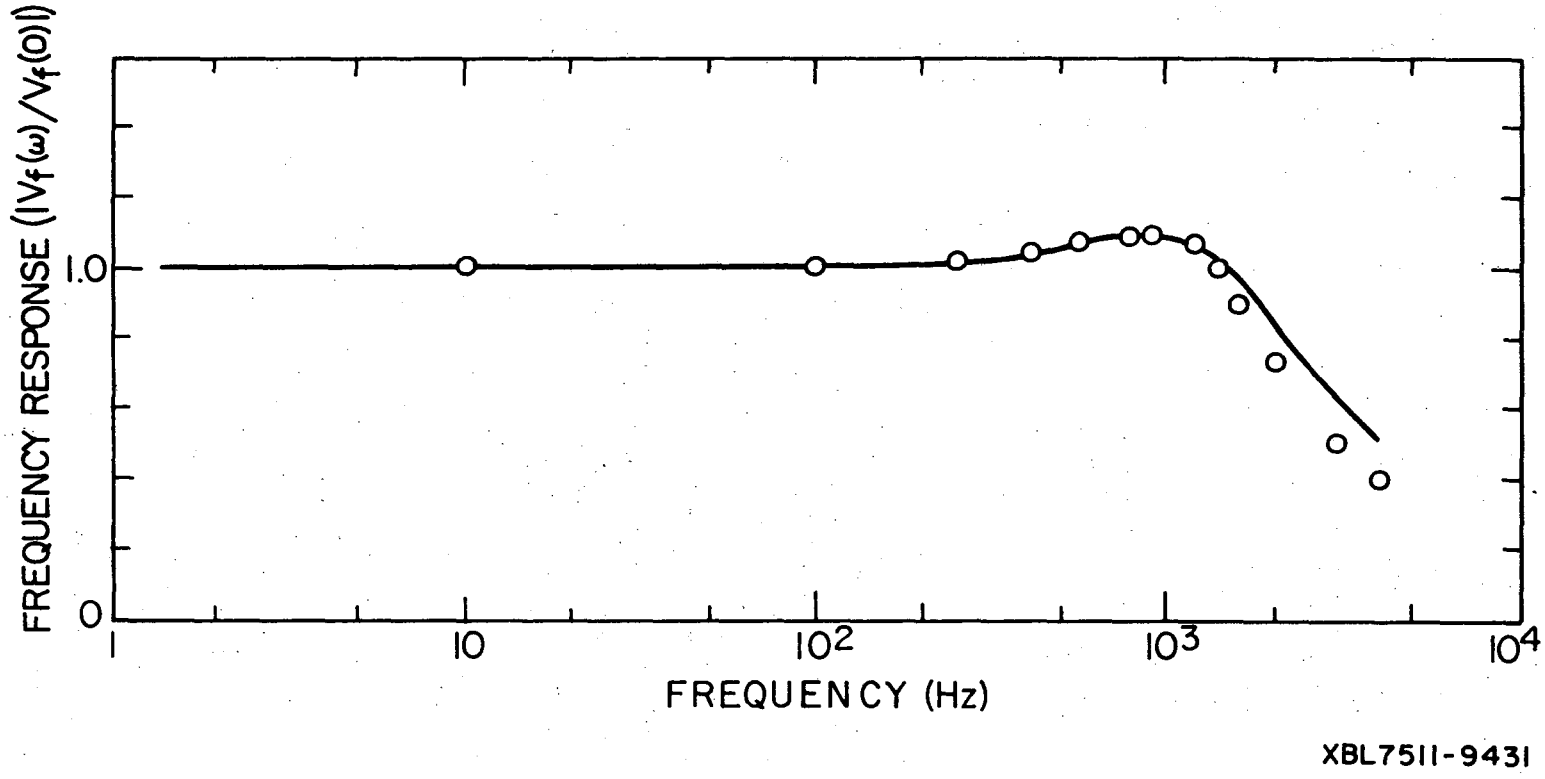
FREQUENCY RESPONSE (|Vf(ω)/Vf(0)|)
1.0
0
1
10
10^2
10^3
10^4
FREQUENCY (Hz)
XBL7511-9431

Fig. 8

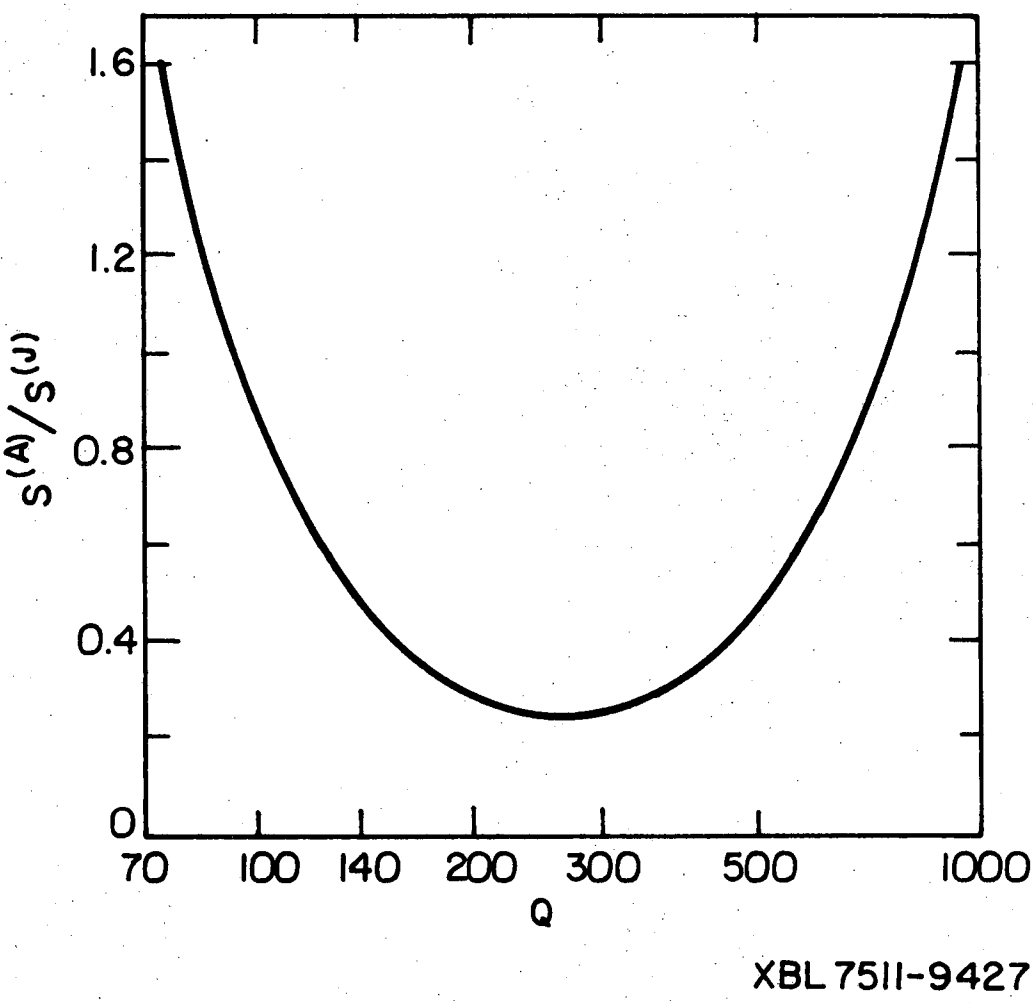

Fig. 9

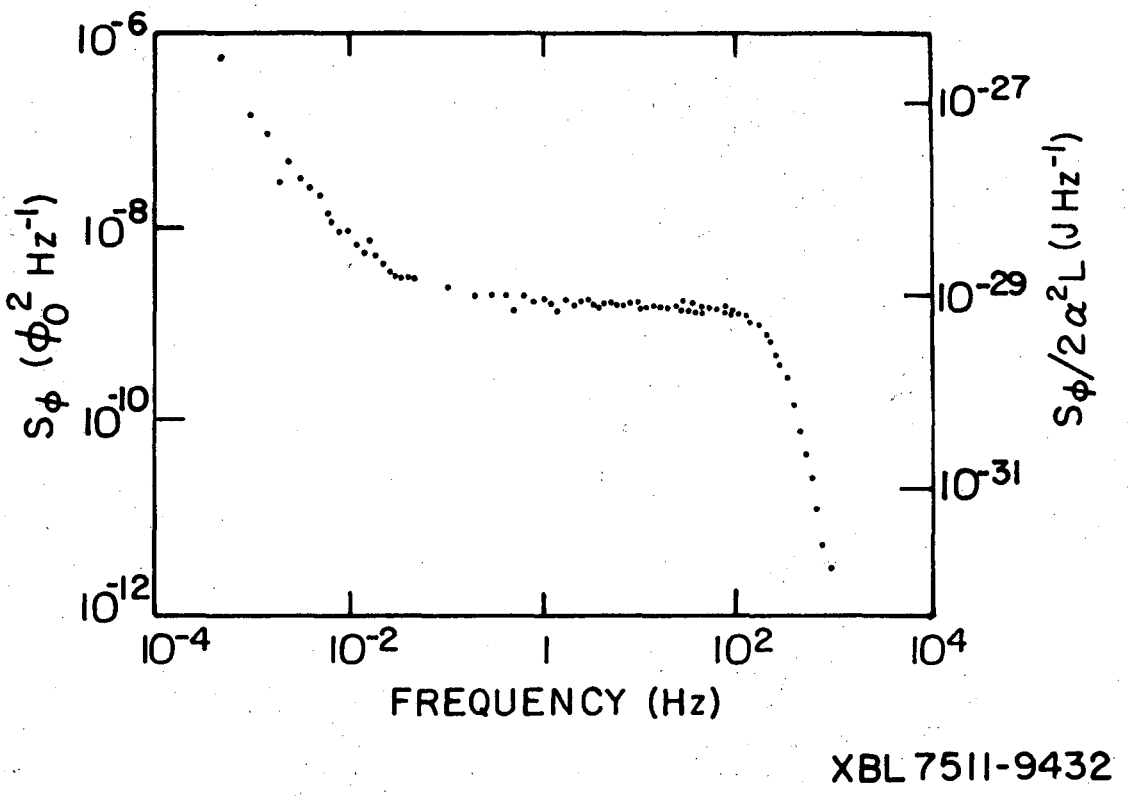
10^{-6}
10^{-8}
10^{-10}
10^{-12}
S_ϕ (ϕ_0^2 Hz^{-1})
10^{-27}
10^{-29}
10^{-31}
$S_\phi/2\alpha^2L$ (J Hz^{-1})
10^{-4}
10^{-2}
1
10^{2}
10^{4}
FREQUENCY (Hz)
XBL 7511-9432

Fig. 10

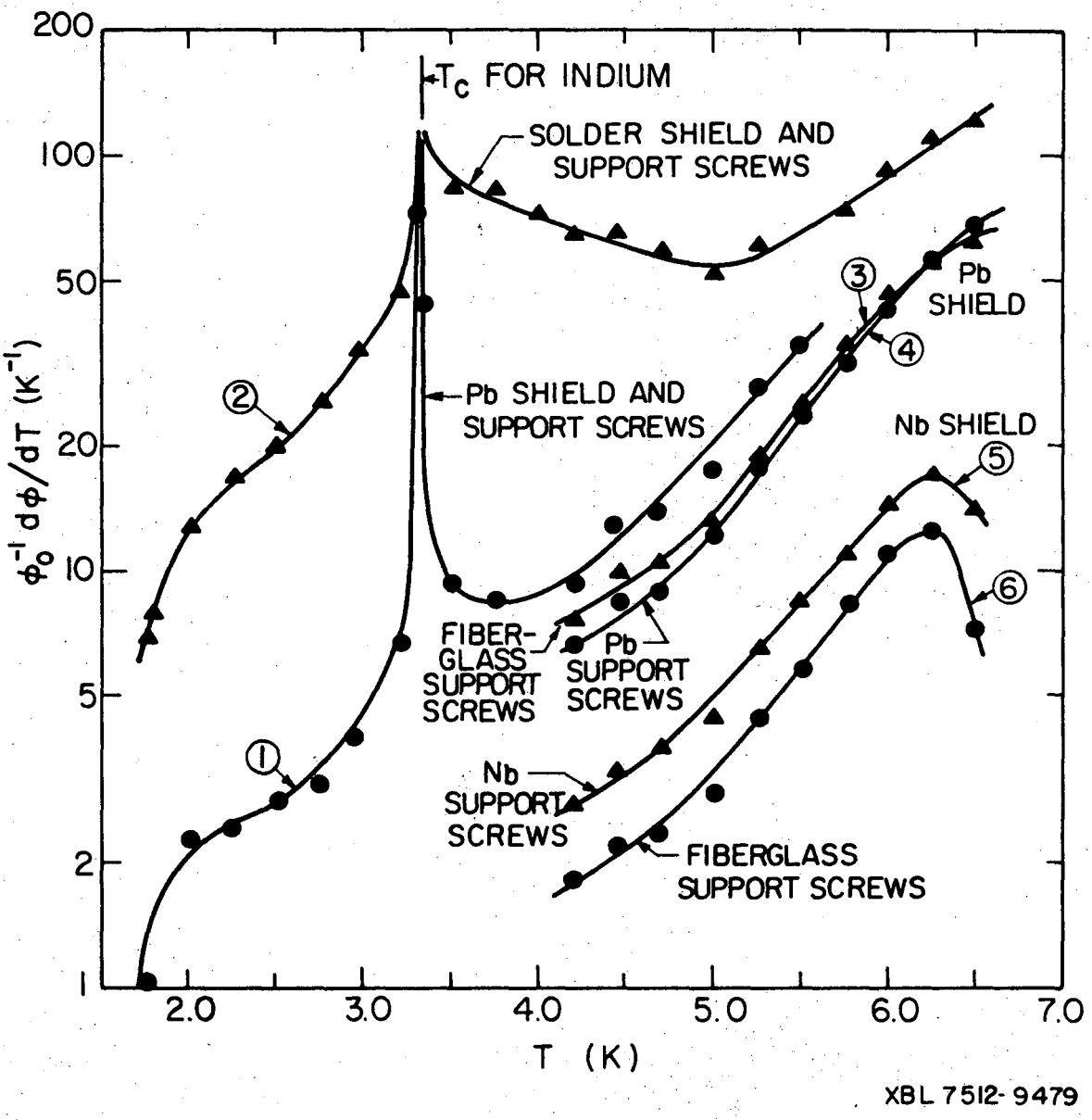

Fig. 11

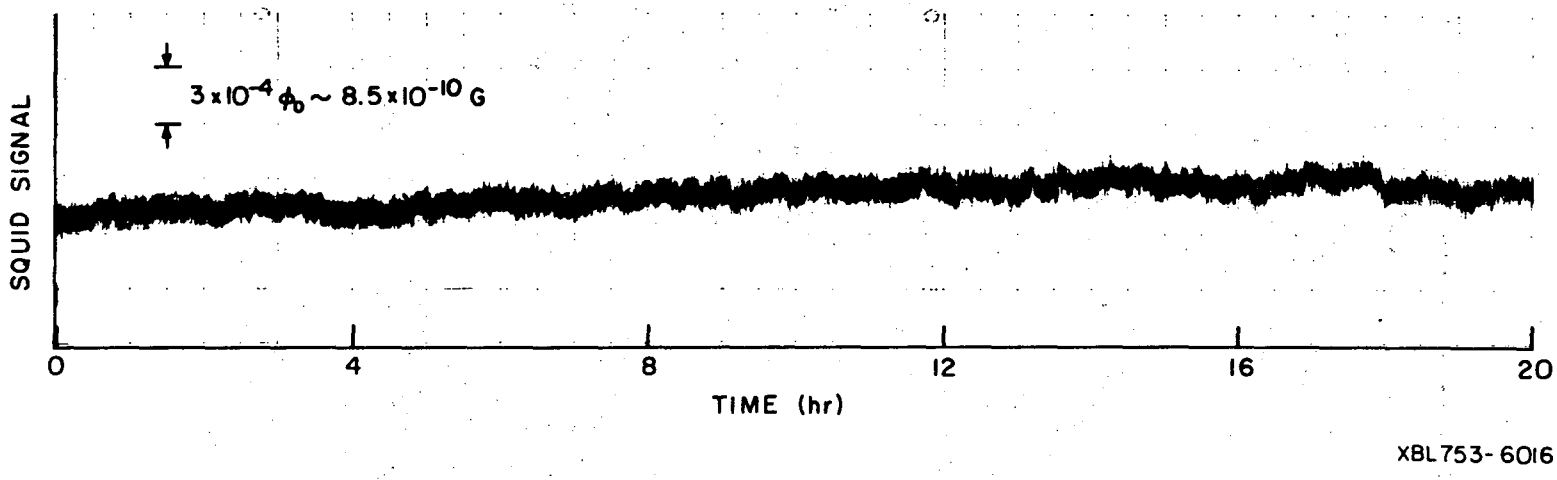
SQUID SIGNAL
$3 \times 10^{-4} \phi_0 \sim 8.5 \times 10^{-10}$ G
0
4
8
12
16
20
TIME (hr)
XBL753-6016

Fig. 12

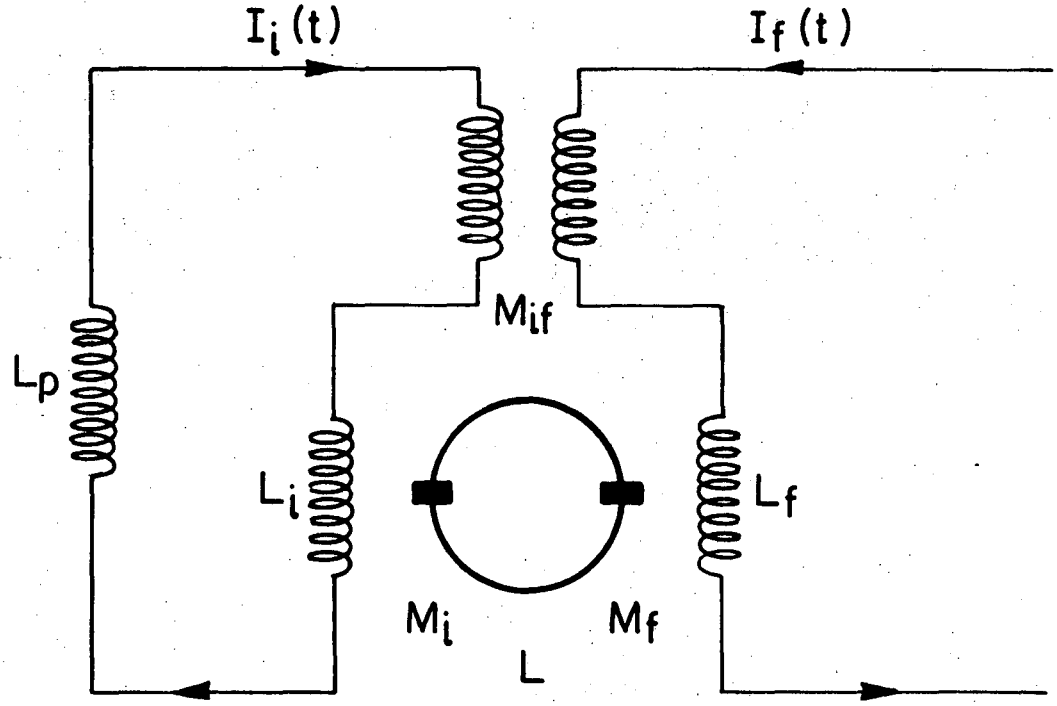

Fig. 13

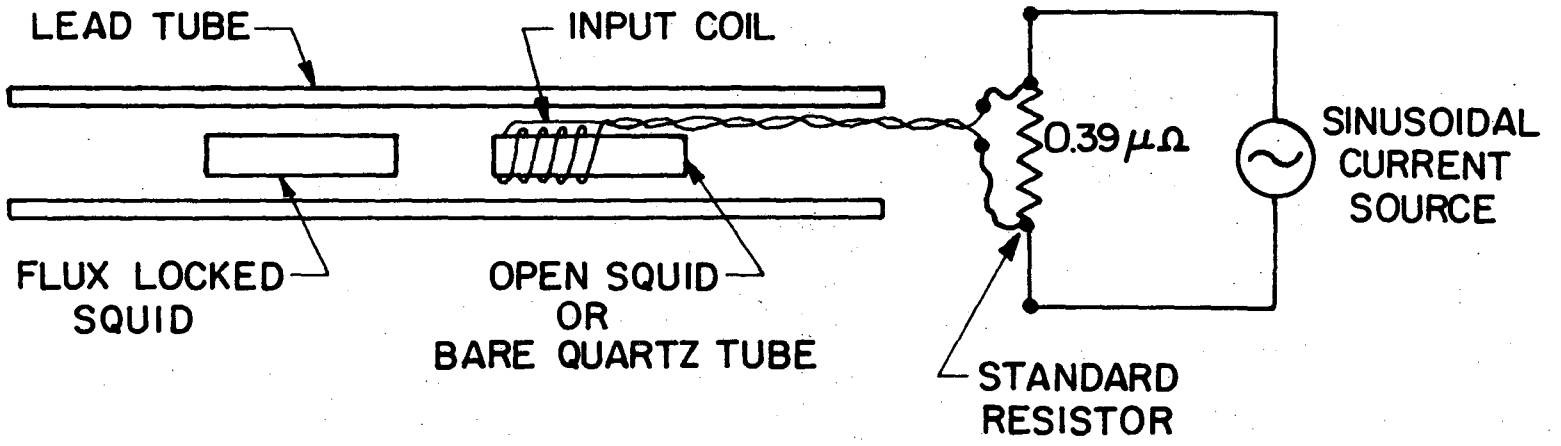
LEAD TUBE
INPUT COIL
0.39 μΩ
SINUSOIDAL CURRENT SOURCE
FLUX LOCKED SQUID
OPEN SQUID OR BARE QUARTZ TUBE
STANDARD RESISTOR
XBL7512-9481

Fig. 14

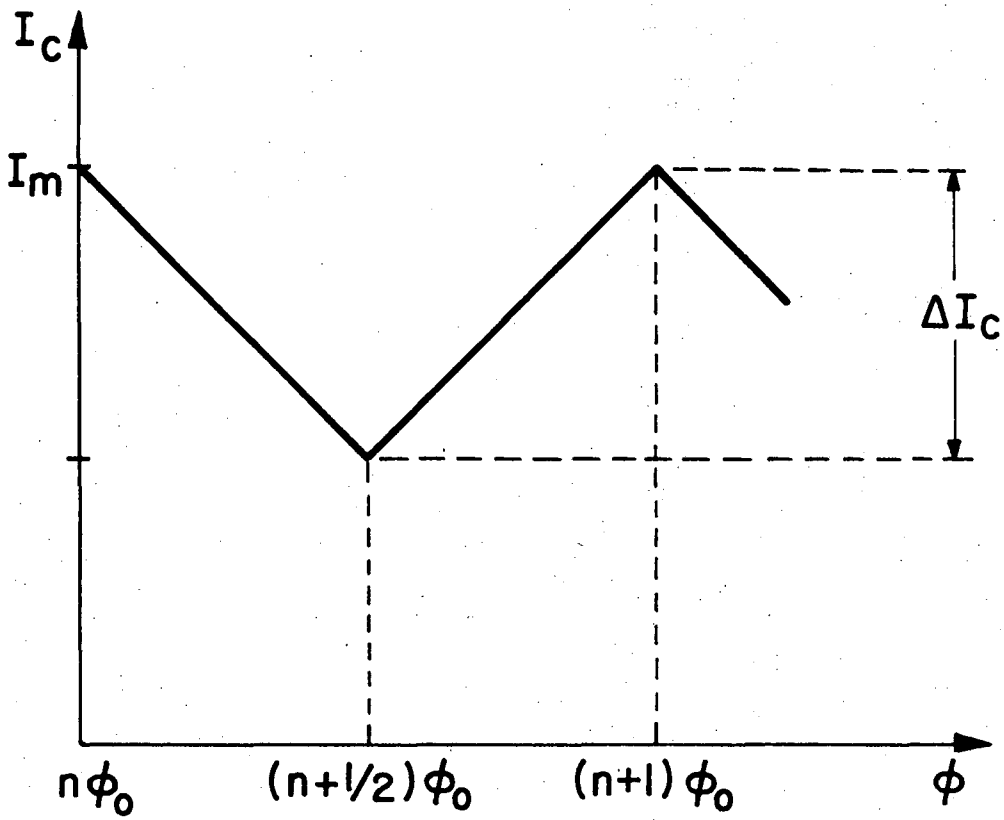

XBL 7512-9482

Fig. 15

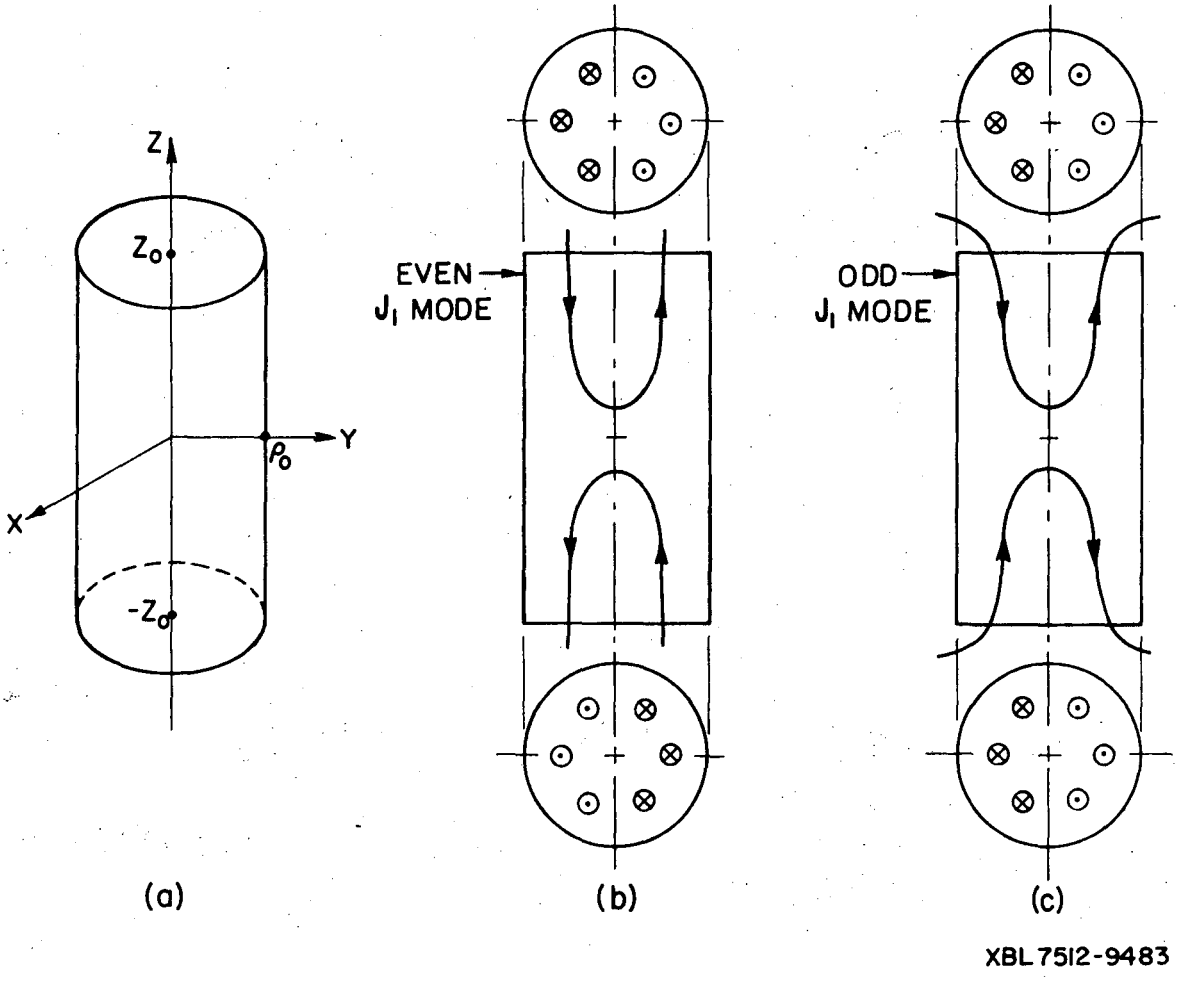

Fig. 16

TECHNICAL INFORMATION DIVISION
LAWRENCE BERKELEY LABORATORY
UNIVERSITY OF CALIFORNIA
BERKELEY, CALIFORNIA 94720